ELSEVIER

Coordination Chemistry Reviews
182 (1999) 19–65

COORDINATION CHEMISTRY REVIEWS

Phosphoraneiminato complexes of transition metals

Kurt Dehnicke *, Matthias Krieger, Werner Massa

Fachbereich Chemie der Philipps-Universität Marburg, Hans-Meerwein-Straße, D-35032 Marburg, Germany

Received 20 March 1998; accepted 17 July 1998

Contents

Abstract

A review on syntheses, chemical reactions, structure and bonding of phorphoraneiminato complexes of transition metals (TM) is given. The ligand group $[NPR_3]^-$, not known as a discrete ion, is isoelectronic with, amongst others, $[OSiMe_3]^-$, and is capable of a versatile coordination chemistry. Apart from terminal functions $[M] \equiv N-PR_3$ with a close to linear M–N–P axis (**A**) and bent axis

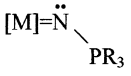

(**B**), complexes with μ_2-N-bridges forming symmetrical (**D**) or unsymmetrical (**C**) four-membered M_2N_2 rings are as well known as those of the μ_3-N-type (**E**) leading to heterocubane

* Corresponding author. Tel.: +49-6421-282031; Fax: +49-6421-288917.

PII: S0010-8545(98)00191-X

M_4N_4 structures. The coordination type preferred is primarily dependent on the oxidation state (OS) of the TM, but also on the ligand sphere of the TM and on the steric and electronic properties of the substituents at phosphorus (R = organic group, NR'_2, halogen). Types **A** and **B** are predominantly realized in complexes of metals in high OS. Electron-rich metals prefer type **E**, and in mediate OS bonding modes **C** and **D** prevail.

Keywords: Phosphoraneiminato complexes; Transition metals; Oxidation states

1. Introduction

Transition metal (TM) phosphoraneiminato complexes are compounds containing the NPR_3^- ligand moiety. The R groups at the phosphorus atoms represent organic substituents, and, albeit only seldom, halides or NR_2 groups. The NPR_3^- ligand is isoelectronic with a variety of ligands, the most prominent examples being silyl imido complexes $[M] \equiv NSiR_3$ and silyloxy complexes $[M] \equiv OSiR_3$, Scheme 1.

A discrete NPR_3^- ion is yet unknown, and even in alkali metal derivatives such as $[(LiNPPh_3 \cdot LiBr)_2 \cdot 4THF]$ [1a] with heterocubane structure or in $MNPPh_3$ with M = Li [1b], Na [2], K [3] X-ray crystal structures reveal hexameric molecular aggregates which are soluble in toluene. In contrast, numerous compounds in which this ligand group is coordinated with main group elements and transition metals exhibit strongly covalent element-nitrogen bonds. Very recently, phosphoraneiminato complexes of main group (MG) elements have been reviewed [4]. In a review given in 1989 [5] the NPR_3^- ligand was characterized only as a terminally bound function of types **A** and **B** (Scheme 2). Numerous examples with μ_2-N- and μ_3-N-bridging NPR_3-functions have since been disclosed. Thus, the coordination chemistry of phosphoraneiminato complexes has developed into a broad area of research comprising even compounds with cluster-like structures.

Bonding mode **A** implies a (σ, 2π) set of orbitals for the metal–nitrogen triple bond, comparable to those in η^5-cyclopentadienyl complexes, giving rise to a Ψ-isolobal relationship between these ligands. With both NPR_3^- and Cp^- ligands bearing one formal negative charge, structural and bonding features of these ligands in complexes of the same transition metal can be related. Quantum mechanical calculations [6] have been carried also out since the field of phosphoraneiminato chemistry has last been reviewed.

The bonding mode chosen is predominantly affected by the oxidation state (OS) of the TM (Scheme 2): metal centres in high OS, i.e. metal atoms with empty d-orbitals prefer type **A**, those in low OS type **E**. Examples with two different

	CPR_3^{2-}	NPR_3^-	OPR_3
$CSiR_3^{3-}$	$NSiR_3^{2-}$	$OSiR_3^-$	$FSiR_3$
$NAlR_3^{3-}$	$OAlR_3^{2-}$	$FAlR_3^-$	

Scheme 1.

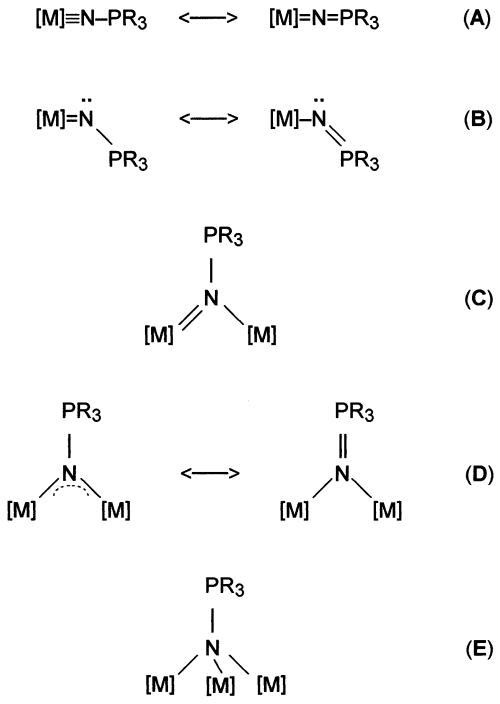

Scheme 2.

bonding modes, e.g. **A**/**B** or **A**/**D**, are found in complexes with medium OS. Furthermore, the nature and number of other ligand atoms at the metal centre, as well as the steric demands and inductive effects of the groups R bound to phosphorus effect the bonding mode. For this review we have chosen to cover TM phosphoraneiminato complexes ordered by decreasing OS of the metal centres (Sections 2–9). In Section 10, aspects of bonding in TM phosphoraneimine complexes are discussed.

Some phosphoraneiminato complexes, especially those of titanium and of the rare earth elements, have proven to be highly efficient catalysts for the polymerization of olefins, as well as for the ring opening polymerisation of lactones [7]. Furthermore, the application of organometallic phosphoraneiminato complexes in C–C-bond forming reactions with carbon electrophiles is an area which is only very recently elaborated in our laboratories [8,9].

2. Oxidation state +VIII (Os)

Formation of osmium(VIII) complex $[OsO_2(NPPh_3)_2(OSiMe_3)_2]$ containing both the isoelectronic ligands $NPPh_3^-$ and $OSiMe_3^-$ by the reaction of osmium tetroxide with $Me_3SiNPPh_3$ has been reported by Roesky et al. [10]:

$$OsO_4 + 2Me_3SiNPPh_3 \rightarrow [OsO_2(NPPh_3)_2(OSiMe_3)_2] \quad (1)$$

An X-ray structural analysis of the product has not been carried out, yet it can be assumed that the oxo-ligands are placed *cis* to each other which is typical of transition metals with d^0-configuration.

3. Oxidation state + VII (Re)

Reaction of dirhenium heptoxide with (*N*-trimethylsilyl) triphenylphosphoraneimine has been reported to yield the monomeric phosphoraneiminato complex $[ReO_3(NPPh_3)]$ and hexamethylsiloxane, according to Eq. (2) [11]:

$$Re_2O_7 + 2Me_3SiNPPh_3 \rightarrow 2[ReO_3(NPPh_3)] + O(SiMe_3)_2 \quad (2)$$

In the course of later examinations employing P-ethylderivative $Me_3SiNPEt_3$ it has been found out that an analog P-ethyl complex $[ReO_3(NPEt_3)]$ is formed in good yield, but also Re(V) donor–acceptor complex $[Re(O)(OSiMe_3)_3(Me_3SiNPEt_3)]$ [12].

In analogy, the difunctional phosphoraneimine $C_2H_4(PPh_2NSiMe_3)_2$ with *cisoid* $P=NSiMe_3$ groups [13] gives rise to the non-cyclic $[(ReO_3NPPh_2)_2C_2H_4]$ with *transoid* configuration [11]. The Re–N–P angles are significantly smaller (154.1° in average) than those found in $[ReO_3(NPPh_3)]$ which are 162.0° in average [12], Fig. 1. It should be noted that structural parameters of P-ethyl derivative $[ReO_3(NPEt_3)]$ [12] resemble very much those found in the P-phenyl complex $[ReO_3(NPPh_3)]$. In all the complexes the Re–N bond lengths are in the range of double bonds, corre-

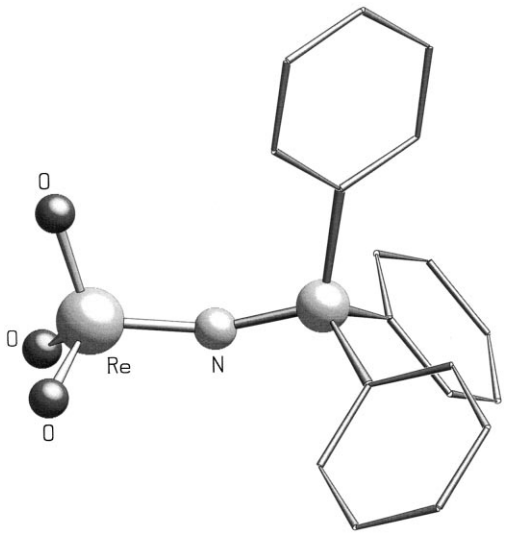

Fig. 1. Molecular structure of $[ReO_3(NPPh_3)]$ [12].

Table 1
Selected bond lengths (pm) and bond angles (°) in phosphoraneiminato complexes of rhenium(VII)

	Re–N	P–N	ReNP	Ref.
$[ReO_3(NPPh_3)]$	179.3(7)	158.9(7)	162.0(5)	[11]
$[ReO_3(NPEt_3)]$	178.6(4)	160.0(4)	160.6(2)	[12]
$[(ReO_3NPPh_2)_2C_2H_4]$	180.6(6)	157.2(7)	154.1(3)	[11]
$[4\text{-}CF_3C_6H_4\overline{CNPPh_2NReO_2N}]_2$	202.8(13), 212.8(12)	161.1(12),165.6(15)	125.3(8)	[15]

sponding to bonding mode **A** (Table 1). The reaction of Re_2O_7 with $CH_2(PPh_2NSiMe_3)_2$ [14], does also not lead to the formation of a cyclic rhenium derivative [11]. However, a cyclic structure based on a centrosymmetric Re_2N_2 four-membered ring with trigonal–bipyramidal coordination at the rhenium atoms is formed in $[4\text{-}CF_3C_6H_4\overline{CNPPh_2NReO_2N}]_2$ [15], corresponding to bonding mode **C**.

4. Oxidation state +VI (Mo, W, Re)

The monomeric tungsten complexes $[WF_4(NPR_3)_2]$ (R = Me [16] and Ph [17]), $[WCl_5(NPPh_3)]$ and $[WCl_4(NPPh_3)_2]$, as well as $[WCl_5(NPCl_2NPCl_3)]$ have been known for some time [5]. They are derived from the corresponding tungsten hexahalides. Halogen-substituted tungsten phosphoraneiminato complexes of the type $[WCl_5(NPCl_3)]$ and *cis*-$[WCl_4(NPCl_2Ph)_2]$ have been synthesized by the reactions of WCl_6 with the phosphoraneimines $Cl_2RP=NSiMe_3$ (R = Cl or Ph) [18]. Complexes $[WCl_5(NPCl_3)]$ and *cis*-$[WCl_4(NPCl_2Ph)_2]$ differ in that $[WCl_5(NPCl_3)]$ realizes a short W–N distance (177.3 pm) and an almost linear W–N–P axis (176.2°), whereas W–N bonds in *cis*-$[WCl_4(NPCl_2Ph)_2]$ are longer (181.5 and 182.3 pm) and the W–N–P arrays are more strongly bent (162.0 and 158.5°). Thus, bonding modes of the phosphoraneiminato moieties can be referred to as belonging to type **A** in $[WCl_5(NPCl_3)]$, but rather **B** in *cis*-$[WCl_4(NPCl_2Ph)_2]$. The appealing ion pair $[Cl_3Ga–Cl–WCl_4(NPCl_3)]$ (Fig. 2) is formed in an attempt to transform $[WCl_5(NPCl_3)]$ into the cationic complex $[WCl_4(NPCl_3)]^+$ by the action of gallium trichloride [18]. An attack by the Lewis acid $GaCl_3$ leads to a tremendous enlargement of the W–Cl bond in $[Cl_3Ga\text{-}Cl–WCl_4(NPCl_3)]$ (270.4 pm), which has been decisively long in the starting material $[WCl_5(NPCl_3)]$ already (237.7 pm) since the chloro function is placed *trans* to the $NPCl_3^-$ ligand $[WCl_5(NPCl_3)]$. Therefore, the bonding mode changes from **A** to **B**, along with the reduction of the W–N–P bond angle to 156.2°.

Substitution of more than two halide functions cannot be achieved employing the silylated reagents Me_3SiNPR_3. Contrary to this, the course of reaction of $Me_3SiNPPh_3$ with tungsten nitride chloride or tungsten dioxo dichloride in acetonitrile solutions are outlined in Eqs. (3) and (4), respectively [19]:

$$WNCl_3 + 4Me_3SiNPPh_3 \rightarrow [W(NPPh_3)_4]^{2+} 2Cl^- + ClSiMe_3 + N(SiMe_3)_3 \quad (3)$$

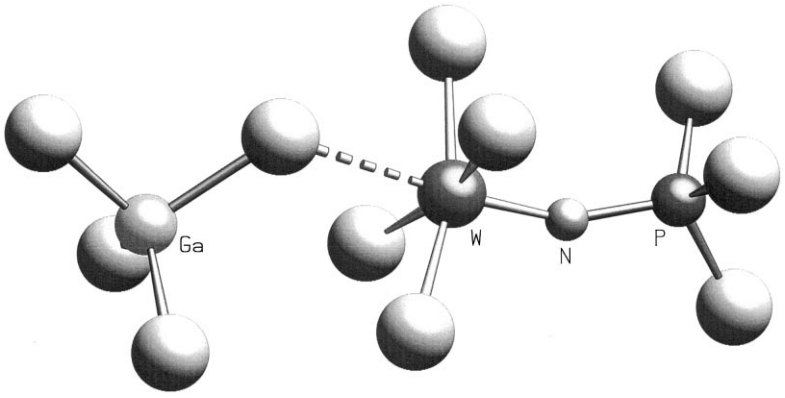

Fig. 2. Molecular structure of the ion pair $[Cl_3Ga–Cl–WCl_4(NPCl_3)]$ [18].

$$WO_2Cl_2 + 4Me_3SiNPPh_3 \rightarrow [W(NPPh_3)_4]^{2+} 2Cl^- + 2O(SiMe_3)_2 \quad (4)$$

In the dicationic $[W(NPPh_3)_4]^{2+}$ the tungsten atom is surrounded by a slightly distorted tetrahedron of nitrogen atoms of the $NPPh_3^-$ ligands, the W–N distances being 180.9 pm in average, corresponding to W=N double bonds. The W–N–P bond angles vary from 157 to 163°, giving rise to bonding mode **A**. The tungsten atom is perfectly shielded by the P-phenyl substituents, as revealed by X-ray crystal structure determination [19], Fig. 3.

Application of Eq. (3) to $MoNCl_3$ yields the analogous $[Mo(NPPh_3)_4]^{2+}$ ion, which, together with the counter ion $[Mo(\equiv N)Cl_3(NPPh_3)]^-$ constitutes the first

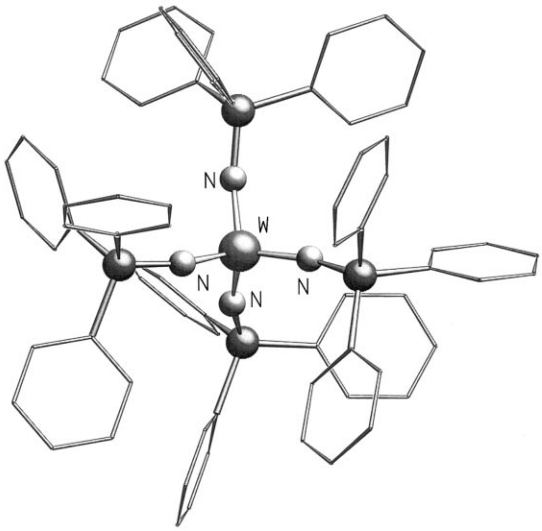

Fig. 3. View of the dication $[W(NPPh_3)_4]^{2+}$ in the structure of $[W(NPPh_3)_4]Cl_2$ [19].

Table 2
Selected bond lengths (pm) and bond angles (°) in phosphoraneiminato complexes of Mo(VI), W(VI), and Re(VI)

		M–N	P–N	MNP	Ref.
$[Mo(NPMe_3)_4]Cl_2$		177.5–184.0(10)	159.5–162.4(10)	142.8–170.2(7)	[21]
$[Mo(NPPh_3)_4]^{2+}$	Cation:	176.9–180.0(9)	159–161.6(9)	149.9–172.8(6)	[20]
$[Mo(N)Cl_3(NPPh_3)^-]_2$	Anions:	185.4(9), 184(1)	159.5(9), 159(1)	138.0(5), 145.3(8)	
$[Mo(N)(NPPh_3)_3]$		193(1)	157(1)	137(1)	[98]
$[WCl_5(NPCl_3)]$		177(2)	158(2)	176.2(12)	[18]
$[Cl_3GaClWCl_4(NPCl_3)]$		175(2)	161.6(14)	156.2(11)	[18]
$[WCl_4(NPCl_2Ph)_2]$		181.5(5), 182.3(5)	157.7(5), 156.5(6)	162.0(3), 158.5(3)	[18]
$[W(NPPh_3)_4]Cl_2$		179.4–182.5(8)	156.4–160.8(8)	157.0–163.3(5)	[19]
$[ReNCl(NPPh_2C_6H_4)]_2$		193-201(1)[br] [b]	164(1)	123.0(6)[a] [a], 150.0(7)[a]	[22]

[a] a, in average.
[b] br, bridging group.

phosphoraneiminato complexes of molybdenum in the OS + VI [20]. The structure of the dication is analogous to that of $[W(NPPh_3)_4]^{2+}$. The anions can be derived structurally from the $[Mo(\equiv N)Cl_4]^-$ ion with tetragonal pyramidal structure [20] by replacing one chloro function by a $NPPh_3^-$ ligand. Interestingly, the substitution of Ph by Me imparts only a marginal effect on the bonding parameters in the dication, as shown by the crystal structure analysis of $[Mo(NPMe_3)_4]Cl_2$ [21] (Table 2). The Mo–N–P angles in the P-phenyl derivative are reduced to 152.5° (P–Me complex 161.7°), with the Mo–N distances virtually unchanged (180.7 pm in $[Mo(NPMe_3)_4]Cl_2$; 178.9 pm in P–Ph derivative; average values). The neutral Mo(VI) phosphoraneiminato complex $[Mo(N)(NPPh_3)_3]$ has been synthesized only very recently in our laboratories, namely by the action of the lithio derivative $LiNPPh_3$ [1b] upon $[Mo(N_3S_2)Cl_3]_2$, [98].

Cyclometallaphosphazene complexes of the type $[Cl_3\overline{WNPPh_2CHPPh_2N}]$ or $[F_3\overline{WNPPh_2NPPh_2N}]$ and related compounds were reviewed some time ago [40] and are not discussed here in detail.

In an attempt of synthesizing the trication $[Re(NPPh_3)_4]^{3+}$, being isoelectronic with $[W(NPPh_3)_4]^{2+}$, by the reaction of $ReNCl_4$ with $Me_3SiNPPh_3$ according to Eq. (3), Re(VII) was reduced to Re(VI), giving the ortho-metallation product $[Re(N)Cl(NPPh_2C_6H_4)]_2$ [22] (Fig. 4), in which the two rhenium atoms are linked by the nitrogen atoms of the two $(NPPh_2C_6H_4)_2^{2-}$ ligands, thereby forming a non-planar Re_2N_2 four-membered ring with a Re–Re distance of 268.1 pm. This observation and the diamagnetism of the complex are suggestive of a Re–Re bond. The two terminal nitrido ligands are placed *cis* in a so far [23,24] unknown arrangement [22].

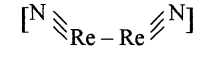

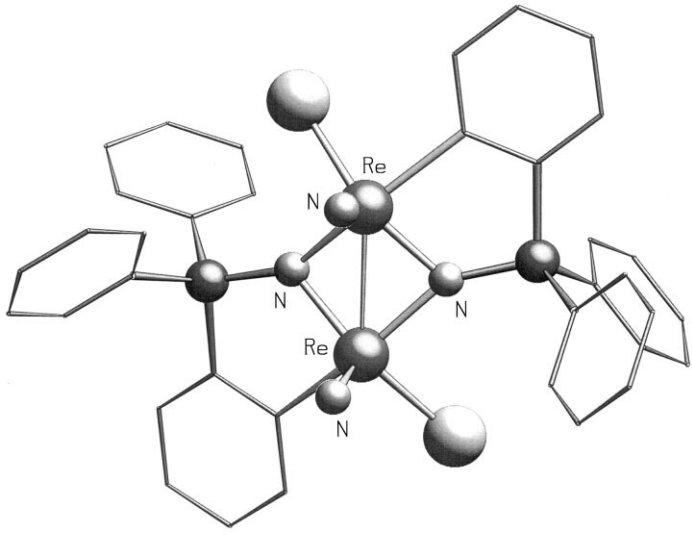

Fig. 4. Molecular structure of $[Re(N)Cl(NPPh_2C_6H_4)]_2$ [22].

5. Oxidation state +V (V, Nb, Ta, Mo)

All group V elements in their highest OS form stable phosphoraneiminato complexes, in which the NPR_3^- ligand realises without exception terminal bonding modes with short metal–nitrogen distances. This is equally true of the less well-known examples of molybdenum(V) with d^1-configuration and of rhenium(V) with d^2-configuration (Table 3).

The conspicuous features of the two complexes $[VOF_2(NPPh_3)]$ [25] (Fig. 5) and $VOCl_2(NPPh_2NS(O)Me_2]$ [26], which can be prepared from VOF_3 and $VOCl_3$, respectively, are the small V–N–P bond angles of 137.4° (132.9°). Thus, they represent bonding mode **B**. A very interesting synthetic route for phosphoraneiminato complexes of vanadium(V) devised by Doherty et al. makes use of the high reactivity of the monomeric imido complex $VCl_3(NSiMe_3)$ [27], which reacts smoothly with triorganophosphorus dichlorides along with cleavage of the trimethylsilyl function [28], Eq. (5):

$$[VCl_3(NSiMe_3)] + PCl_2R_3 \rightarrow [VCl_4(NPR_3)] + ClSiMe_3$$

$$\text{where } R_3 = Ph_3,\ Ph_2Me,\ PhMe_2,\ Me_3. \qquad (5)$$

Lewis bases such as acetonitrile, THF, or chloride ions, can be added to the supposedly monomeric complexes $[VCl_4(NPR_3)]$. The P-phenyl derivative $[VCl_4(NPPh_3)]$ is converted stepwise to $[VCl_3(NPR_3)_2]$ and $[VCl_2(NPR_3)_3]$ by treatment with $Me_3SiNPPh_3$ [28]. Surprisingly, the compounds so formed are prone to react with dry ammonia in dichloromethane forming the homoleptic complex $[V(NPPh_3)_4]^+Cl^-$ with vanadium coordinated in a tetrahedral fashion (Fig. 6) [28]. It can be assumed that the V–N bond lengths of 176.0–177.6 pm are enlarged due

Table 3
Selected bond lengths (pm) and bond angles (°) in phosphoraneiminato complexes of V(V), Nb(V), Ta(V), Mo(V), and Re(V)

	M–N	P–N	MNP	Ref.
$[VOF_2(NPPh_3)]$	172.7(4)	161.6(5)	137.4(3)	[25]
$[VOCl_2(NPPh_2NS(O)Me_2]$	171.6(3)	163.3(3)	132.9(2)	[26]
$[V(NPPh_3)_4]^+Cl^-\cdot 4CH_3CN$	176.0–177.6(6)	155.7–158.0(5)	141.0–177.0(3)	[28]
$[NbCl_4(NPPh_3)]_2$	177.6(8)		171.1(6)	[29]
$[(\eta^5\text{-}C_5EtMe_4)NbCl_3(NPPh_3)]$	183.4(3)	160.0(3)	168.5(2)	[30]
$[\{(\eta^5\text{-}C_5EtMe_4)NbCl_3(NPPh_2)\}_2C_2H_2]$	183.7(3)	159.5(3)	172.8(2)	[30]
$[ONbCl_3NPPh_2(CH_2)_2PPh_2NNbCl_3]$	180.7(3)		160.4(2)	[31]
$[NbCl_4(NP^iPr)(CH_3CN)]$	178.2(3)	164.0(3)	165.2(2)	[32]
[Na(15-crown-5)][$NbF_5(NPPh_3)$]	185.7(7)	157.9(3)	165.9(5)	[33]
$[PPh_3NH_2][NbF_5(NPPh_3)]$	184.6(3)	158.2(7)	169.9(2)	[33]
$[NbCl_3(NPPh_3)_2]$	182.7(4); 183.0(6)	160.2(5); 159.5(6)	156.4(3); 161.9(3)	[34]
$[NbCl_3(NP^iPr_3)_2]$	183.5(7); 185.3(9)	156.4(9); 159.0(7)	168.5(5); 168.2(4)	[32]
$[TaCl_4(NPPh_3)]_2$	180.1(8)	159.3(9)	176.8(7)	[35]
$[TaCl_4(NP^iPr_2)]_2$	177.1(9)	163.5(9)	174.7(6)	[32]
$[(\eta^5\text{-}C_5Me_5)TaCl_3(NPPh_2NS(O)Me_2)]$	184.8(3)	159.6(3)	175.1(3)	[26]
$[TaCl_3(NP^iPr_3)_2]$	183.5(6); 185.5(6)	159.4(7); 156.3(6)	169.0(4); 170.4(4)	[32]
$[Ta(NPPh_3))_4]^+[TaCl_6]^-$	186; 184[a]	157; 160[a]	167; 154[a]	[6]
$[MoCl_4(NPPh_3)]_2$	172.3(4)	165.6(4)	168.4(3)	[36]
$[MoCl_4(NPPh_3)(pyridine)]$	171.9(9)	165.3(9)	176.6(6)	[37]
$[MoCl_4(NPPh_3)(OPPh_3)]$	189.7(9)	156.5(9)	169.9(6)	[38]
$[Re(SPh)_4(NPPh_3)]$	174.3(7)	163.4(9)	163.1(6)	[39]

[a] Average values in each of the two crystallographically independent individuals.

to steric hindrance imposed by the phosphoraneiminato moieties, compared with shorter V–N distances in mono(phosphoraneiminato) complexes of V(V) described above.

Phosphoraneiminato complexes of Nb, Ta, Mo, and Re in the OS + V are easily accessible from their chlorides or fluorides by treatment with silylated phosphoraneimines. In all examples characterized by X-ray crystallography the NPR_3^- ligands are bound terminally featuring short metal–nitrogen bonds with M–N double bond character and the M–N–P bond angles being rather large, values ranging from 156 to 177° (Table 3). In our terminology, they can therefore be classified as belonging to type **A** compounds.

Complexes with association via halogen bridges, such as $[NbCl_4(NPPh_3)]_2$ [29], can be dissociated upon exposure by donor molecules (e.g. CH_3CN or Ph_3PO) with the formation of well-defined 1:1 complexes, in which the donor molecule is generally placed *trans* to the phosphoraneiminato N-atom. The strong *trans*-influence of the short M–N bonds gives rise to long M–donor atom distances. As an example, Nb-(NP^iPr) distances are 178.2 pm in average in $[NbCl_4(NP^iPr_3)(CH_3CN)]$, Nb–(NC–$CH_3$) being 239.7 pm long, Fig. 7 [32].

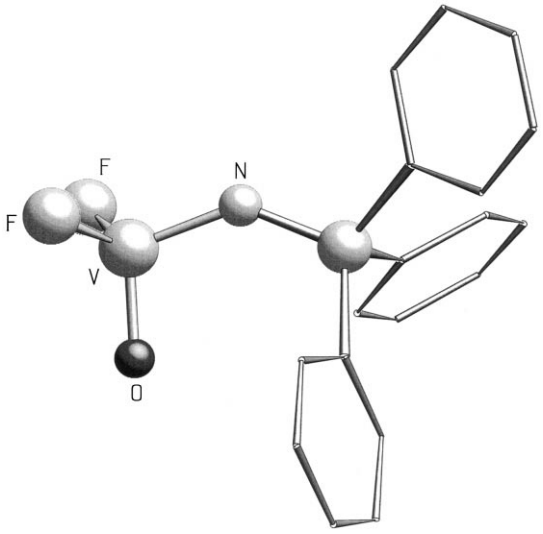

Fig. 5. Molecular structure of $[VOF_2(NPPh_3)]$ [25].

The bis(phosphoraneiminato) complexes $[NbCl_3(NPPh_3)_2]$ [34] and $[TaCl_3(NP^iPr_3)_2]$ [32] possess monomeric molecular structures with distorted trigonal–bipyramidal coordination at the metal centres. With view of the spatial demand of the phosphoraneiminato moieties and the short M–N bond lengths, the NPR_3^- ligands occupy equatorial positions in these complexes, Fig. 8. Attempts to prepare a tantalum analog of $[NbCl_3(NPPh_3)_2]$ by reacting $[TaCl_5]_2$ with

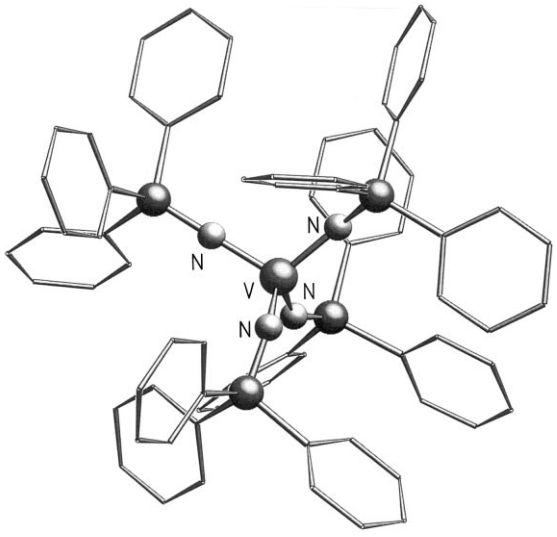

Fig. 6. View of the cation $[V(NPPh_3)_4]^+$ in the structure of $[V(NPPh_3)_4]Cl$ [28].

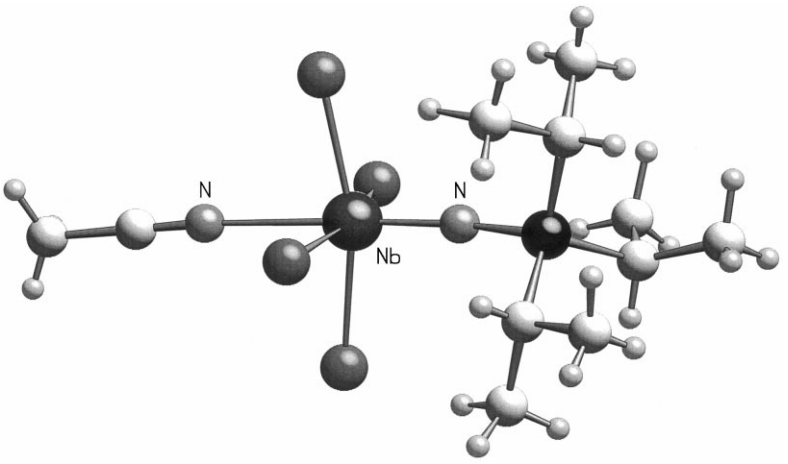

Fig. 7. Molecular structure of $[NbCl_4(NP^iPr_3)(CH_3CN)]$ [32].

$Me_3SiNPPh_3$ lead to spontanous rearrangement to give the ionic complex $[Ta(NPPh_3)_4]^+[TaCl_6]^-$, Fig. 9 [6].

The homoleptic cation is isoelectronic with the tungsten(VI) dication $[W(NPPh_3)_4]^{2+}$, see above. Ab-initio calculations on hypothetical $[Ta(NPH_3)_4]^+$ are in good agreement with the short Ta–N bond lengths which are interpreted as Ta–N double bonds but do not support the Ta–N–P angles. Experimental values for the latter are, in average, 167 and 154°, whereas calculated angles suggest linearity [6].

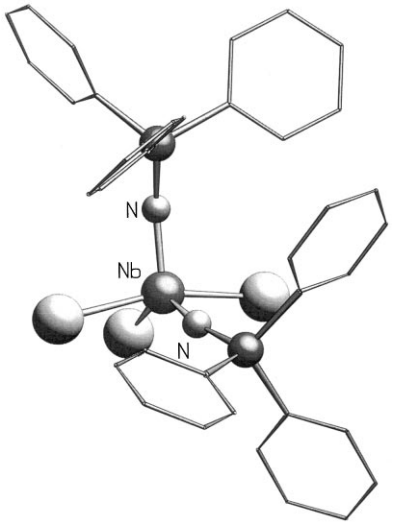

Fig. 8. Molecular structure of $[NbCl_3(NPPh_3)_2]$ [34].

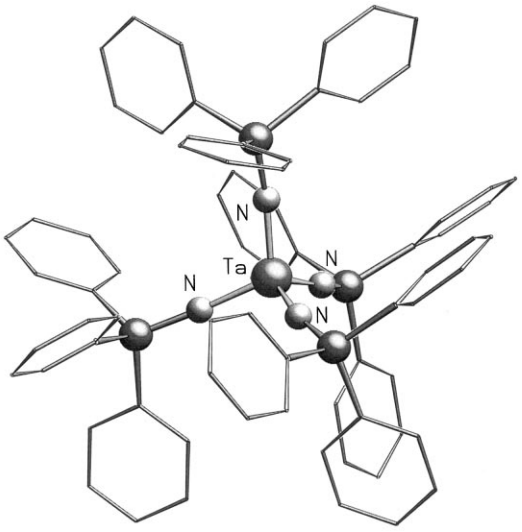

Fig. 9. View of the cation $[Ta(NPPh_3)_4]^+$ in the structure of $[Ta(NPPh_3)_4][TaCl_6]$ [6].

Five-fold coordination at the metal centre is observed also in the structure of the rhenium complex $[Re(SPh)_4(NPPh_3)]$ [39]. It should be noted that in this complex the $NPPh_3^-$ ligand prefers the apical position of a tetragonal pyramid in which the four thiophenolate groups and the Re atom are unable to form a common plane.

Starting from neutral phosphoraneiminato complexes, addition of the fluoridation agent NaF in the presence of 15-crown-5 in acetonitrile suspension can bring about conversion into anionic phosphoraneiminato complexes as outlined in Eq. (7) [33]:

$$[NbCl_4(NPPh_3)(CH_3CN)] + 5NaF + 15\text{-}C\text{-}5 \rightarrow [Na(15\text{-}C\text{-}5)][NbF_5(NPPh_3)] + 4NaCl + CH_3CN \quad (7)$$

Complex $[Na(15\text{-}C\text{-}5)][NbF_5(NPPh_3)]$ consists of an ion pair held together by two Na···F contacts which are made possible by the sodium ion coordinated by the five oxygen atoms of the crown ether molecule (Fig. 10) [33].

The Cl/F ligand exchange reactions of phosphoraneiminato complexes of Mo(V) and W(VI) proceed via different routes. In boiling acetonitrile PPh_3F_2 is formed according to Eq. (8) [41]:

$$[MoCl_4(NPPh_3)(CH_3CN)] + 5NaF + 15\text{-}C\text{-}5 \rightarrow PPh_3F_2 + \text{‘}[Na(15\text{-}C\text{-}5)][MoNF_3]\text{’} + 4NaCl + CH_3CN \quad (8)$$

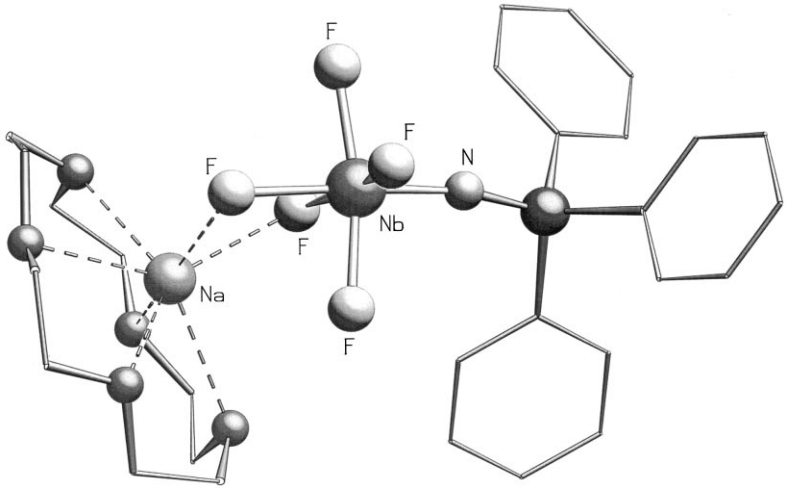

Fig. 10. Structure of the ion pair $[Na(15\text{-}C\text{-}5)][NbF_5(NPPh_3)]$ [33].

6. Oxidation state +IV (Ti, Zr, Hf, V, Ru, U)

Phosphoraneiminato complexes of Ti(IV) are well known. They can be obtained by the reaction of the corresponding titanium halide with silylated phosphoraneimines. Mono-substitution is achieved without difficulty at room temperature, but harsher reaction conditions are needed for the introduction of a second NPR_3^- moiety. Higher substitution is not attainable using this synthetic strategy. Homoleptic tetrakis(triphenylphosphoraneiminato)titanium, however, has been synthesized in toluene solution by the action of organolithiums starting from $[TiCl_2(NPPh_3)_2]$, Eq. (9) [42]:

$$[TiCl_2(NPPh_3)_2] + LiR \rightarrow [Ti(NPPh_3)_4] + \ldots \text{ where } R = Me,\ Cp \qquad (9)$$

In most examples with bulky substituents (e.g. phenyl) at the phosphorus atom monomeric molecular structures are obtained (Table 4). In contrast, P-alkyl derivatives have been found to dimerize in the solid state and thus the unsymmetric Ti_2N_2 four-membered rings formed are of bonding mode **C**. Raising the degree of substitution above one may result in the formation of cluster-like structures, as shown by the ionic complex $[Ti_3Cl_6(NPMe_3)_5]^+$ [45]. The Ti_2N_2 rings of dimeric complexes $[TiCl_3(\mu\text{-}NPR_3)]_2$ ($R_3 = Me_3$, Et_3, Me_2Ph; type **C**) are apt to cleavage by the action of solvent molecules. For example, reaction of $[TiCl_3(NPEt_3)]_2$ with tetrahydrofurane gives monomeric $[TiCl_3(NPEt_3)(THF)_2]$ [46], whereas weaker Lewis-basic acetonitrile reacts with $[TiCl_3(NPMe_2Ph)]_2$ to give a species $[TiCl_2(\mu\text{-}Cl)(NPMe_2Ph)(CH_3CN)]_2$ [48] which is dimerized via chloro bridges. Presumably, the Lewis-acidity of these complexes constitutes the reason for high catalytic activity in olefin polymerization reactions [7].

Table 4
Selected bond lengths (pm) and bond angles (°) in phosphoraneiminato complexes of Ti(IV), Zr(IV), Hf(IV), V(IV), Ru(IV), and U(IV)

	M–N	P–N	MNP	Ref.
$[TiCl_3(NPPh_3)]$	171.9(4)	161.4(4)	180	[43]
$[TiCl_3(NPPh_3)(TiCl_4)]_2$	171.6(3)	162.6(3)	173.8(2)	[44]
$[TiCl_3(NPMe_3)]_2$	184.3(4), 208.2(4)	164.7(4)	134.9(2), 127.5(2)	[45]
$[TiCl_3(NPEt_3)]_2$	184.7(4), 210.3(4)	165.3(4)	132.6(2), 130.2(2)	[46]
$[TiCl_3(NPEt_3)(THF)_2]$	173.4(3)	161.1(3)	160.0(2)	[46]
$[TiCl_3\{NPPh_2NPPh_2N(SiMe_3)_2\}]$	172.1(3)	162.3(3)	177.5(2)	[47]
$[TiCl_2(\mu\text{-}Cl)(NPMe_2Ph)(CH_3CN)]_2$	173.9(3)	161.4(3)	156.4(2)	[48]
$[Ti_2Cl_5(NPMe_2Ph)_3]$	175.6(5)$^{t\ a}$, 199.2(4)$^{br\ b}$, 180.4(4)^{br}, 194.4(4)^{br}, 234.6(4)^{br}	159.6(5)^{t}, 161.4(4)^{br}	156.1(3)^{t}	[45]
$[Ti_3Cl_6(NPMe_3)_5]^+[BPh_4]^-$	205.7(8)–232.8(9)	156(1)–164.3(8)	124.6(4)–142.2(5)	[45]
$[Ti_3Cl_8(NPMe_3)_3]^+Cl^-$	194.7(5)(μ_2-N), 210.1(4)(μ_3-N), 213.6(5)(μ_3-N)	162.6(6)	137.9(1)(μ_2-N), 127.9(2)(μ_3-N), 125.7(3)(μ_3-N)	[49]
$[TiF_3(NPPh_3)(HNPPh_3)]_2$	177.7(4)	157.2(4)	174.3(3)	[50]
$[CpTiCl_2(NPPh_3)]$	178(1)		174.7(9)	[51]
$[CpTiCl_2(NPMe_3)]$	174.6(3)	158.6(3)	170.7(2)	[45]
$[CpTiCl_2(NPPh_2NS(O)Me_2)]$	176.4(2)	159.5(2)	158.7(1)	[26]
$[Cp^*TiCl_2(NPPh_2NHSiMe_3)]$	178.1(3)	158.1(3)	166.4(1)	[47]
$[TiCl_2(NPPh_3)(\mu\text{-}OMe)]_2$	174.8(5)	158.1(6)	165.3(4)	[52]
$[TiCl_2(NPPh_3)_2]$	179.0(3)	156.8(3)	166.6(2)	[48]
$[Ti(NPPh_3)_4]$	186.9(4), 187.6(3)	155.4(4), 154.8(4)	149.3(3), 151.4(3)	[42]
$[Zr_2Cl_4(NPMe_3)_4(\mu\text{-}HNPMe_3)]$	194.6(2)^{t}, 213.9(2)–216.2(3)^{br}	158.1(3), 159.3(3)^{t}, 163.3(3), 163.8(2)^{br}	159.3(2), 155.6(2)^{t}	[55]
$[Zr_3Cl_6(NPMe_3)_5]^+$, $[Zr_2Cl_6(NPMe_3)_3]^-$	216(1)(μ_2-N)$^{a\ c}$, 226.5(9)(μ_3-N)^{a}, 215(1)(μ_2-N)^{a}	159(2)–161.9(9)	132.9(7)(μ_2-N), 126.1(6)(μ_3-N), 133.6(7)(μ_2-N)	[56]
$[Hf_3Cl_6(NPMe_3)_5]^+$, $[Hf_2Cl_7(NPMe_3)_2]^-$	215(1)(μ_2-N), 223.6(9)(μ_3-N), 212(1) (μ_2-N)	159(1)–164.6(9)	133.1(8)(μ_2-N), 125.9(6)(μ_3-N), 132.6(8)(μ_2-N)	[56]
$[VCl_3(NPMe_2Ph)(PMe_2Ph)_2]$	175.4(5)	160.4(5)	163.7(3)	[57]
$[VCl_3(NPMe_2Ph)(PMe_2Ph)_2]\cdot H_2O$	167.5(20)	164(2)	169.4(13)	[57]

Table 4 (*Continued*)

	M–N	P–N	MNP	Ref.
$[VCl_3(NPPh_3)(OPPh_3)]$	168.9(7)	161.5(7)	161.4(4)	[58]
$[V_3Cl_6(NPMe_3)_5^+]_2$, $[V_4O_4Cl_8(NPMe_3)_2]^{2-}$	173(2)–181(2)^{t}, 203.5(14)–208(2)^{br}, 184(2)^{br}, 201(2)^{br}	159(2)–164(2), 161(2)	148.5(11)-153.8(13)^{t}, 124.5(8)-129.6(7)^{br}, 138.0(9), 128.8(9)	[59]
$[V_2^{III/IV}Cl_4(NPPh_3)_3]$	173.1(4)^{t}, 186.4(4)–206.6(4)^{br}	158.9(4), 160.7(4), 161.9(4)	172.1(3)^{t}, 132.2(2)–138.0(2)	[49]
$[RuCl_3(NPEt_2Ph)(PEt_2Ph)_2]$	184.1(3)	158.6(3)	174.9(3)	[60]
$[UCp_3(NPPh_3)]$	207(2)	161(2)	172(1)	[61]

[a] t, terminal group.
[b] br, bridging group.
[c] a, in average.

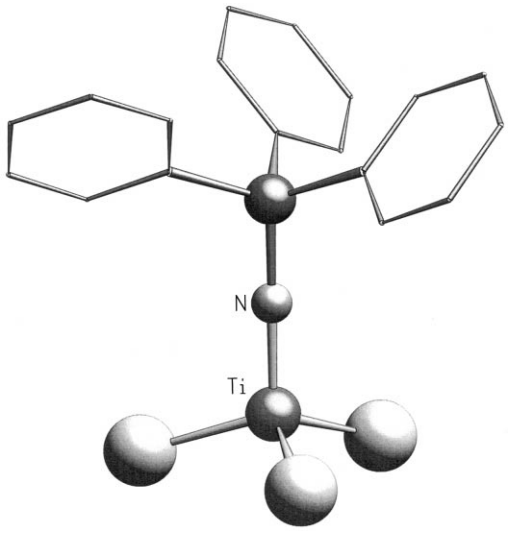

Fig. 11. Molecular structure of $[TiCl_3(NPPh_3)]$ [43].

The Ti–N bond lengths of the terminally bonded NPR_3^- groups correspond to shortened double bonds indicative of type **A**. Therefore, titanium phosphoraneiminato complexes of this type may serve as model compounds to illustrate the Ψ-isolobal relationship with cyclopentadienyl complexes. Among the shortest Ti–N distances are those found in monomeric $[TiCl_3(NPPh_3)]$ (mean value 171.9 pm, [43]). It is also the only example containing an entirely linear Ti–N–P axis (Fig. 11), though the latter is due to the TiNP entity being placed around a three-fold crystallographic axis (space group $R\bar{3}$). The Ti–O–Si axes of the two symmetry-independent molecules of isoelectronic $[TiCl_3(OSiPh_3)]$ have been determined also to be close to linearity (176.1 and 167.0°, space group $P2_1/c$ [43]). $[TiCl_3(NPPh_3)]$ forms a dimeric molecular complex $[TiCl_3(NPPh_3)(TiCl_4)]_2$ [44] upon treatment with $TiCl_4$. Despite sixfold coordination of the Ti atom, the Ti–N distances remain equally short (171.6 pm), as does the Ti–N–P axis not deviate much from linearity, the corresponding angle being 173.8° in average, Fig. 12. Significantly longer Ti–N bond lengths are observed in complexes in which the titanium atoms are coordinated by sterically demanding substituents, e.g. Cp or even Cp*. This observation also holds when a second NPR_3^- ligand is present, as can be illustrated by comparison with the Ti–N distances found in the species $[CpTiCl_2(NPPh_3)]$ (178 pm [51]) and $[TiCl_2(NPPh_3)_2]$ (179 pm [48]). Finally, Ti–N bond lengths are enlarged up to 187 pm in $[Ti(NPPh_3)_4]$ [42], which is isoelectronic with $[V(NPPh_3)_4]^+$ (Section 5, Fig. 13). It should be noted that the Ti–N distances in $[Ti(NPPh_3)_4]$ can still be regarded as double bonds as revealed by X-ray structure determination. Moreover, Ti–N–P bond angles indicate the bonding to be of type **B**. Ti–N distances in dimeric complexes $[TiCl_3(NPR_3)]_2$ (R = Me, Et [45,46]) with unsymmetrical Ti_2N_2 rings are only slightly shorter. In these complexes belonging

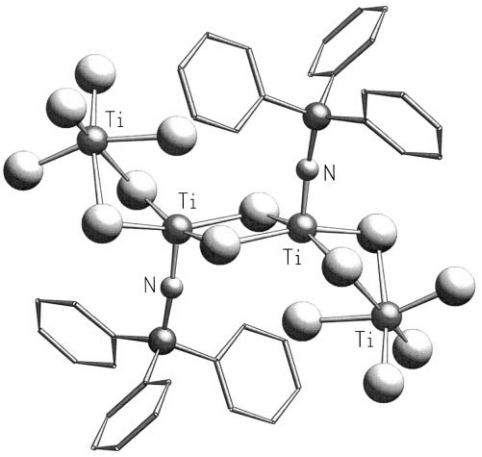

Fig. 12. Molecular structure of the donor-acceptor complex $[TiCl_3(NPPh_3)(TiCl_4)]_2$ [44].

to bonding mode **C** the two longer bonds of the four membered rings are characterized to be of a donor–acceptor nature and are ca. 210 pm in length, Fig. 14. The two different Ti–N bonds result from the trigonal–bipyramidal coordination of the Ti atoms forcing the ligands in axial positions further away from the metal centres. In close analogy Ti–N bonds of the Ti_2N_2 four-membered rings in the isoelectronic silylimido complex $[TiCl_3(NSiMe_3)]_2^{2-}$ [53] differ decisively, the mean values being 177.4 and 200.1 pm. In contrast to this Ti–N bonds in the 1,3-dimethyl-imidazoliniminato complex of titanium, $[TiCl_3(NIm)]_2$ [54], comprising a central Ti_2N_2 four-membered ring, are almost equal in length well (195.8 and 196.2 pm) and they agree quite well with the average Ti–N distances in $[TiCl_3(NPR_3)]_2$ (see above). Degeneration of dimeric complexes $[TiCl_3(NPR_3)]_2$ is

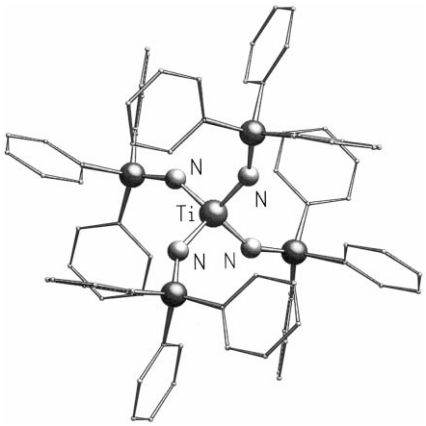

Fig. 13. Molecular structure of $[Ti(NPPh_3)_4]$ [42].

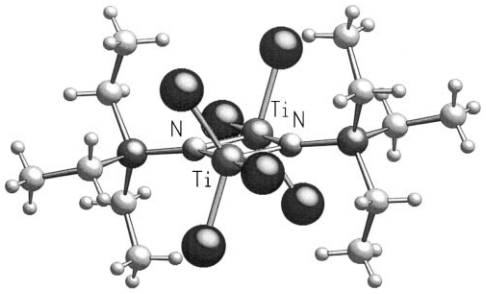

Fig. 14. Molecular structure of $[TiCl_3(NPEt_3)]_2$ [45].

brought about by tetrahydrofuran, yielding monomeric donor–acceptor complexes. In the structure of $[TiCl_3(NPEt_3)(THF)_2]$ [46], one THF molecule is positioned *cis*, and one *trans* to the phosphoraneiminato ligands. The strong *trans*-influence of the $NPEt_3^-$ ligands leads to a long Ti–O bond length in the *trans* position (238.0 pm), being 24 pm longer than the *cis*-Ti–(THF) distance [46]. A completely analogous situation can be observed in the acetonitrile complex $[TiCl_3(NIm)]_2{\cdot}2CH_3CN$ [54], in which both the Ti–acetonitrile distances are 221.2 and 234.3 pm. A *trans*-influence similarly strong can be deduced from strongly differing Ti_2F_2 bridging bonds (194.6 vs 223.3 pm) in the crystal structure of $[TiF_3(NPPh_3)(HNPPh_3)]_2$ ([50] Fig. 15), resulting from the $NPPh_3^-$ ligands in equatorial positions.

The pronounced adaptibility of phosphoraneiminato ligands to various coordination conditions is obvious from the μ_3-bridging function that leads to cluster-like cationic species such as $[Ti_3Cl_6(NPMe_3)_5]^+$ [45], $[Ti_3Cl_8(NPMe_3)_3]^+$ [49] and vanadium(IV) compound $[V_3Cl_6(NPMe_3)_5]^+$ [59] (see below). In these complexes, the metal–nitrogen distances are suggestive of single bonds corresponding to bonding mode **E** (Table 4).

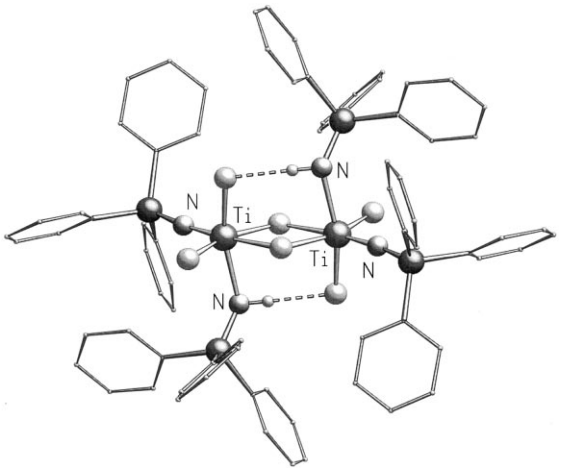

Fig. 15. Molecular structure of $[TiF_3(NPPh_3)(HNPPh_3)]_2$ [50].

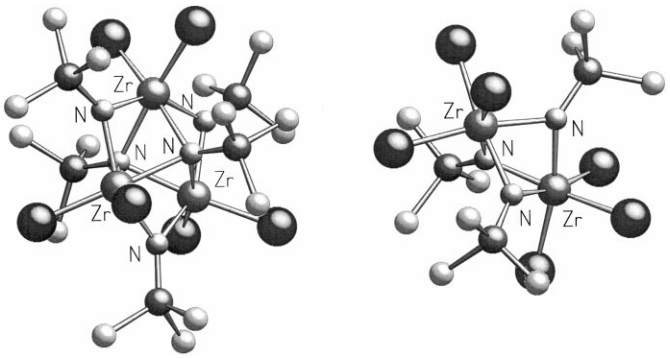

Fig. 16. The structure of $[Zr_3Cl_6(NPMe_3)_5]^+[Zr_2Cl_6(\mu_2\text{-}NPMe_3)_3]^-$ [56].

The most prominent feature of phosphoraneiminato complexes of zirconium and hafnium is the occurence of bridging type **E** and the symmetrical μ_2-N type **D**, being in consistence with the fact that these elements only show a weak tendency to form metal–nitrogen multiple bonds. Furthermore, the synthesis of such complexes requires drastic reaction conditions only realised in the melt with reaction temperatures as high as 220°C and addition of alkali metal fluorides [56], Eq. (10):

$$5ZrCl_4 + 8Me_3SiNPMe_3 + 8NaF \rightarrow [Zr_3Cl_6(NPMe_3)_5]^+[Zr_2Cl_6(NPMe_3)_3]^- + 8FSiMe_3 + 8NaCl \quad (10)$$

Even under these conditions, the P-phenyl derivative $Me_3SiNPPh_3$ does not show any substantial reaction. In the structure of $[Zr_3Cl_6(NPMe_3)_5]^+$ [56] (Fig. 16) the three Zr atoms of the complex cation are linked by two μ_3-N-bridge atoms to form a trigonal–bipyramidal skeleton, the three remaining $NPMe_3^-$ functions being coordinated symmetrically at the edges of the Zr_3-triangle. Zr–N distances of the μ_2-functions are significantly shorter (mean value 216 pm) than those of μ_3-bridging nature (227 pm in average). The trigonal–bipyramidal V_3N_2 cluster skeleton of the corresponding vanadium(IV) compound $[V_3Cl_6(NPMe_3)_5]^+$ [59] is remarkable in that vanadium–vanadium distances are too short to allow for a μ_2-bridging mode of the equatorial $NPMe_3^-$ ligands, which function as terminal ligands of type **B** instead, Fig. 17.

Structural parameters of the Ti complex of the same constitution, $[Ti_3Cl_6(NPMe_3)_5]^+$ [45], have not been solved satisfactorily enough owing to disorder problems. The complex anion $[Zr_2Cl_6(NPMe_3)_3]^-$ [56] consists of two octahedra sharing one common face, i.e. an alignment of two Zr atoms held together by three μ_2-bridging N atoms with Zr–N distances similar in magnitude to those found in the counter-cation (Fig. 16).

Upon varying the molar ratio of reactants in Eq. (10) $[Zr_2Cl_4(NPMe_3)_4(\mu\text{-}HNPMe_3)]$ [55] can be extracted from the cooled melt using acetonitrile as solvent. Surprisingly, two out of four $NPMe_3^-$ ligands assume terminal positions in an almost linear Zr–N–P array of bonding mode **A**, and the short Zr–N bond lengths

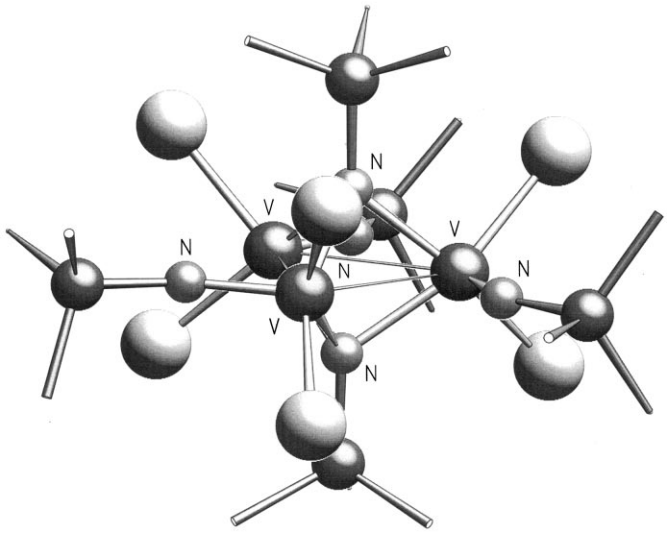

Fig. 17. View of the cation $[V_3Cl_6(NPMe_3)_5]^+$ in the structure of $[V_3Cl_6(NPMe_3)_5^+]_2$-$[V_4O_4Cl_8(NPMe_3)_2]^{2-}$ [59].

(194.6 pm in average) are interpreted as double bonds, see Fig. 18. The phosphoraneiminato ligands are *trans* to the $HNPMe_3$ molecule, the latter binding in a μ_2-bridging fashion giving rise to enlarged Zr–N distances of 243 pm in average.

In the mixed-valence vanadium compound $[V_2^{III/IV}Cl_4(NPPh_3)_3]$ [49] two vanadium atoms are linked by two $NPPh_3^-$ groups. To the butterfly-like V_2N_2 ring thus formed (folding angle 17.3°), the third phosphoraneiminato moiety is bonded terminally, Fig. 19. Not only from the short V–V contacts but also from magnetic measurements it can be assumed that of the three remaining d-electrons, two are used to form a V–V σ-bond whereas the third electron occupies a bonding π-orbital.

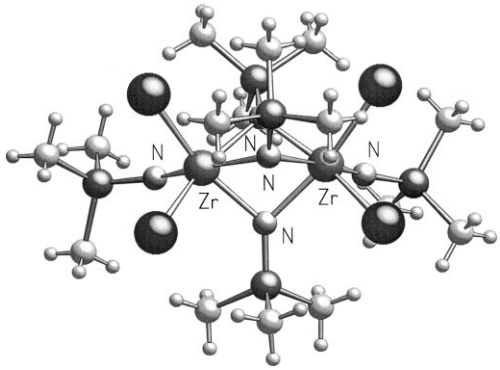

Fig. 18. Molecular structure of $[Zr_2Cl_4(NPMe_3)_4(\mu_2\text{-}HNPMe_3)]$ [55].

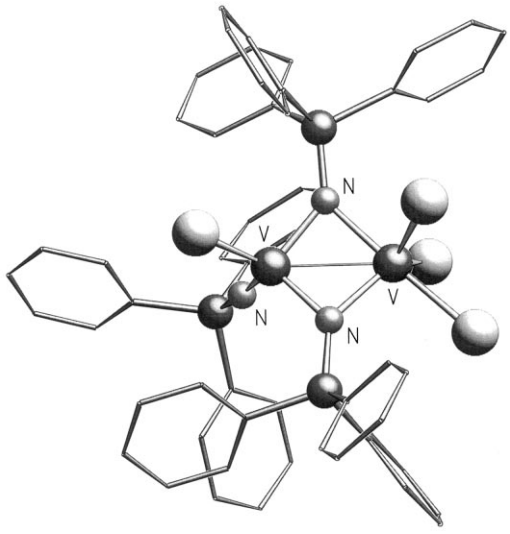

Fig. 19. Molecular structure of the mixed-valence complex $[V_2Cl_4(NPMe_3)_3]$ [49].

Actinides such as thorium and uranium in the OS +IV form monomeric phosphoraneiminato complexes, the metal centres of which are shielded by cyclopentadienyl ligands [61]:

$$AnCp_3Cl + LiNPPh_3 \rightarrow [AnCp_3(NPPh_3)] + LiCl \text{ where } An = Th, U \qquad (11)$$

According to an X-ray structure analysis, the green uranium compound contains the $NPPh_3^-$ ligand as an almost linear U–N–P moiety (bond angle 172°) with a very short U–N bond (207 pm) which is interpreted as a triple bond employing p_π–p_π, d_π–p_π and/or f_π–p_π bonding overlap (Fig. 20).

These observations are supported by extended Hückel molecular orbital calculations carried out using UCp_3NPH_3 as a model [61].

7. Oxidation state +III (Ti, Fe, Rare earth elements)

Phosphoraneiminato ligands complexed to transition metals of oxidation state +III almost entirely bind to two or three metal centres, being consistent with the absence of M–N multiple bonds (Table 5). Only in the rhenium nitrosyl complex $[ReCl_3(NO)(NPPh_3)(OPPh_3)]$ [64] described earlier has a terminally bonded $NPPh_3^-$ ligand of type **B** been observed. Another unexpected exception is found in the sesqui-complexes $[Ln_2Cp_3(NPPh_3)_3]$ (Ln = Y, Dy, Er [65], and Yb [66]), in which one of the $NPPh_3^-$ groups accomplishes type **A** bonding mode, obviously due to steric repulsion by the η^5-cyclopentadienyl ligands.

Only one example has been reported in the case of Ti(III). In diethyl ether as the solvent, $[TiBr_2(NPPh_3)]_2$ [52] is formed at −30°C by the reaction of $[TiCl_3(NPPh_3)]$

with benzylmagnesium bromide which leads to both Cl/Br exchange and reduction of titanium, Eq. (12):

$$2[TiCl_3(NPPh_3)] + 4PhCH_2MgBr \rightarrow [TiBr_2(NPPh_3)]_2 + C_{14}H_{14} + 2PhCH_2MgCl + 2MgCl_2 \quad (12)$$

$[TiBr_2(NPPh_3)]_2$ is a green paramagnetic complex consisting of a centrosymmetric Ti_2N_2 four-membered ring with almost equally long Ti – N distances corresponding to bonding mode **D**, Fig. 21.

Fe(III) derivatives are accessible either by reacting iron trichloride with Me_3SiNPR_3 (R = Ph [62], Et [63]) or by heating phosphoraneimine complex $[FeCl_2(Me_3SiNPEt_3)]_2$ [63] in toluene, in which case the following redox-reaction takes place, Eq. (13):

$$[FeCl_2(Me_3SiNPEt_3)]_2 \rightarrow [FeCl_2(NPEt_3)]_2 + Si_2Me_6 \quad (13)$$

In boiling acetonitrile, synthesis of dimeric acetate complex $[Fe(OAc)_2(NPEt_3)]_2$ can be achieved employing the reaction in Eqs. (13) and (14):

$$2Fe(OAc)_2 + 2Me_3SiNPEt_3 \rightarrow [Fe(OAc)_2(NPEt_3)]_2 + Si_2Me_6 \quad (14)$$

$[Fe(OAc)_2(NPEt_3)]_2$ contains the acetate functions in a chelating manner, untypical of Fe(III) compounds. This leads to a distorted octahedral surrounding at the Fe centres (Fig. 22 [63]), in contrast to the tetrahedral coordination in chloro derivatives $[FeCl_2(\mu_2\text{-}NPR_3)]_2$ (R = Ph [62], Et [63]).

Unusual results have been obtained when examining the reaction of $LiNPPh_3$ [1b] with the well known chloro-bridged bis(cyclopentadienyl)chlorides $[LnCp_2Cl]_2$ (Ln = Y, Dy, Er, Yb) in equimolar amounts. In boiling toluene, readily crystallizing sesqui-complexes $[Ln_2Cp_3(NPPh_3)_3]$ [65] are formed, according to Eq. (15):

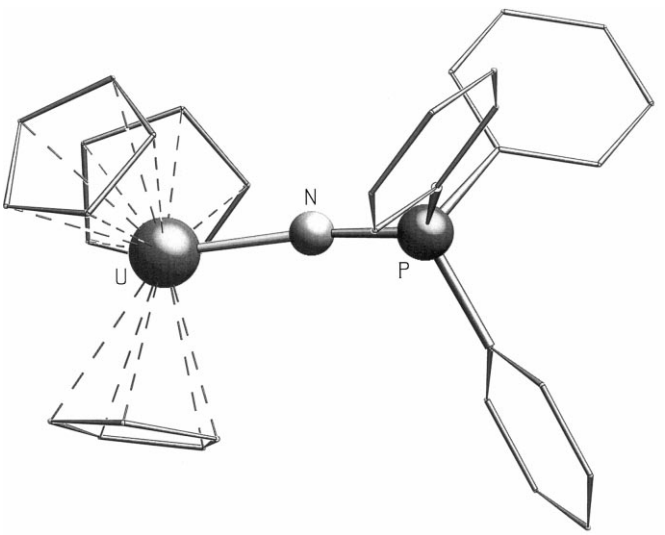

Fig. 20. Molecular structure of $[UCp_3(NPPh_3)]$ [61].

Table 5
Selected bond lengths (pm) and bond angles (°) in phosphoraneiminato complexes of Ti(III), Fe(III), Re(III), Ln(III) (Ln = Y, Ce, Dy, Er, Yb, Sm)

	M–N	P–N	MNP	Ref.
$[TiBr_2(\mu_2\text{-}NPPh_3)]_2$	195.8(3), 196.0(3)	161.0(3)	137.2(2), 139(2)	[52]
$[FeCl_2(\mu_2\text{-}NPPh_3)]_2$	190.1(5), 192.0(6)	160.6(5), 160.9(5)	131.4(3)-139.3(4)	[62]
$[FeCl_2(\mu_2\text{-}NPEt_3)]_2$	191.0(3), 191.7(3)	161.9(3)	136.3(2), 132.8(1)	[63]
$[Fe(O_2C\text{–}CH_3)_2(\mu_2\text{-}NPEt_3)]_2$	195.0(2), 191.9(2)	160.1(2)	130.8(2), 138.3(1)	[63]
$[ReCl_3(NO)(NPPh_3)(OPPh_3)]$	185.5(8)	163.0(8)	138.5(5)	[64]
$[Ln_2(C_5H_5)_3(\mu_2\text{-}NPPh_3)_2(NPPh_3)]$				
Ln = Y	213.9(9)$^{t\ a}$, 227.8-231.7(10)$^{br\ b}$	154.7(8)^{t}, 156.4$^{br,a\ c}$	168.0(6)^{t}, 125.8–136.6(6)^{br}	[65]
Ln = Dy	215.4(7)^{t}, 229.9–233.8(7)^{br}	153.1(7)^{t}, 155.6^{br,a}	167.9(5)^{t}, 125.1–137.7(4)^{br}	[65]
Ln = Er	215.1(9)^{t}, 226.8–228.4(9)^{br}	151.2(10)^{t}, 157.1^{br,a}	169.6(7)^{t}, 125.4–136.7(6)^{br}	[65]
Ln = Yb	214.2(6)^{t}, 226.9–228.7(6)^{br}	150.3(6)^{t}, 155.3^{br,a}	171.1(4)^{t}, 126.4–136.6(3)^{br}	[66]
$[Ln(C_8H_8)Li_3Cl_2(\mu_3\text{-}NPPh_3)_2(THF)_3]$				
Ln = Ce	248.6(4), 247.8(3)	154.9(4), 155.5(4)	134.5(2), 131.8(2)	[1]
Ln = Sm	243.7(4), 242.1(5)	153.6(4), 155.3(4)	135.3(2), 132.8(2)	[1]

[a] t, terminal group.
[b] br, bridging group.
[c] a, in average.

$$3[LnCp_2Cl] + 3LiNPPh_3 \rightarrow [Ln_2Cp_3(NPPh_3)_3] + LnCp_3 + 3LiCl \quad (15)$$

From these solutions, crystals of $[Ln_2Cp_3(NPPh_3)_3]$ are formed as tris-toluene solvates in space group Pbca, regardless of Ln. The metal atoms and the nitrogen atoms of two $NPPh_3^-$ moieties form slightly folded Ln_2N_2 four-membered rings, with the folding angles along the Ln–Ln axes being about 18° (Fig. 23). One metal atom is coordinated with one η^5-Cp ligand as well as one nearly linear $NPPh_3^-$ group, whereas the other Ln atom is surrounded by two η^5-cyclopentadienyl ligands. Ln–N distances of bridging phosphoraneiminato groups are ca. 15 pm longer than those bonded terminally, the latter being the shortest Ln–N bond lengths (Ln = rare earth element) ever observed. It should be stated that the short Ln–N bonds are presumably due to highly polar bonding modes also dicussed in the case of Ln–(η^5-C_5H_5) interactions [67]. Terminally bonded Cp^- and $NPPh_3^-$ ligands give rise to a coordination geometry which deviates only slightly from the one observed at the second type of Ln atom bearing two Cp^- ligands. This is obvious from the N(1)–Ln(1)–Cp(*centroid*) angles being only 4° smaller than the corresponding Cp–Ln(2)–Cp angles. Furthermore, Ln(1)–N(1) distances are very short. These observations are indicative of the Ψ-isolobal relationship between the ligands $NPPh_3^-$ and Cp^-.

Phosphoraneiminato complexes with heterocubane structures are formed from reactions of the lithio derivative $LiNPPh_3$ with η^8-cyclooctatetraenide complexes

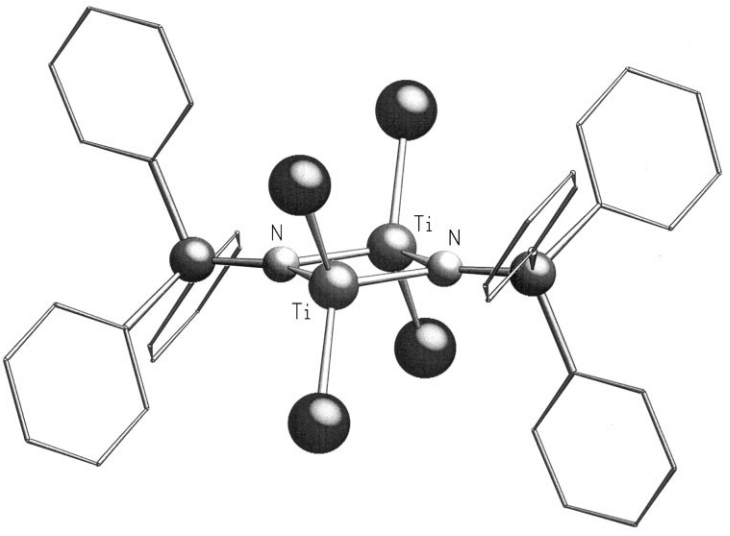

Fig. 21. Molecular structure of $[TiBr_2(NPPh_3)]_2$ [52].

$[Ln(C_8H_8)Cl(THF)_2]_2$ (Ln = Ce, Sm [68,69]) in THF solutions [1b]. As can be seen in Eq. (16), LiCl formed in the course of reaction is incorporated into the heterocubane framework:

$$[Ln(C_8H_8)Cl(THF)_2]_2 + 4LiNPPh_3 + 2LiCl + 2THF \rightarrow 2[Ln(C_8H_8)Li_3Cl_2(NPPh_3)_2(THF)_3] \quad (16)$$

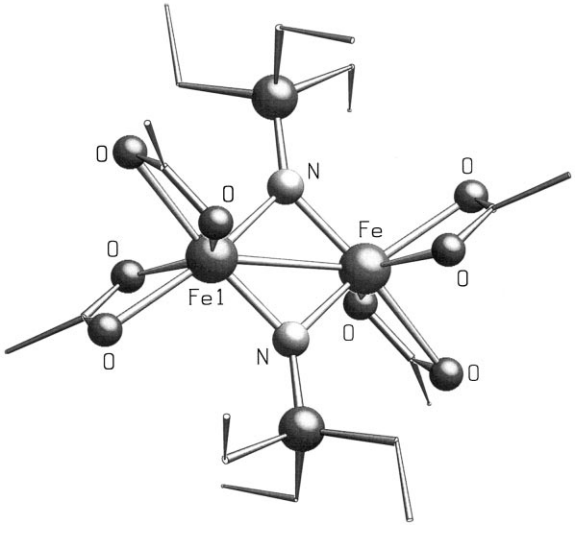

Fig. 22. Molecular structure of $[Fe(O_2C-CH_3)(NPEt_3)]_2$ [63].

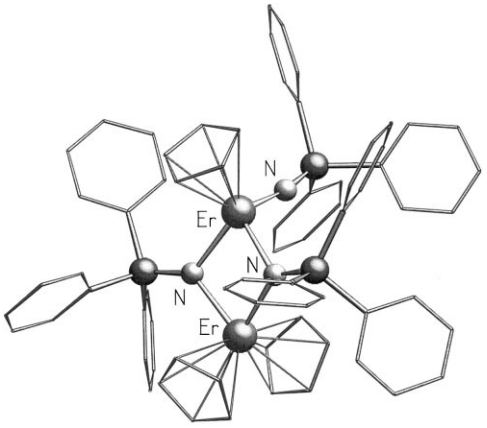

Fig. 23. Molecular structure of $[Er_2Cp_3(NPPh_3)_3]$ [65].

Compounds $[Ln(C_8H_8)Li_3Cl_2(NPPh_3)_2(THF)_3]$ with Ln = Ce, Sm crystallize isotypic in the space group *I*2/*a*, containing three additional THF molecules per formula unit. The heterocubane framework is formed from one Ln, three Li, two Cl and two N atoms of the $NPPh_3^-$ groups, Fig. 24 [1b]. The lanthanoid atoms Ce/Sm are shielded by the η^8-C_8H_8 ring, and the Li atoms by THF molecules.

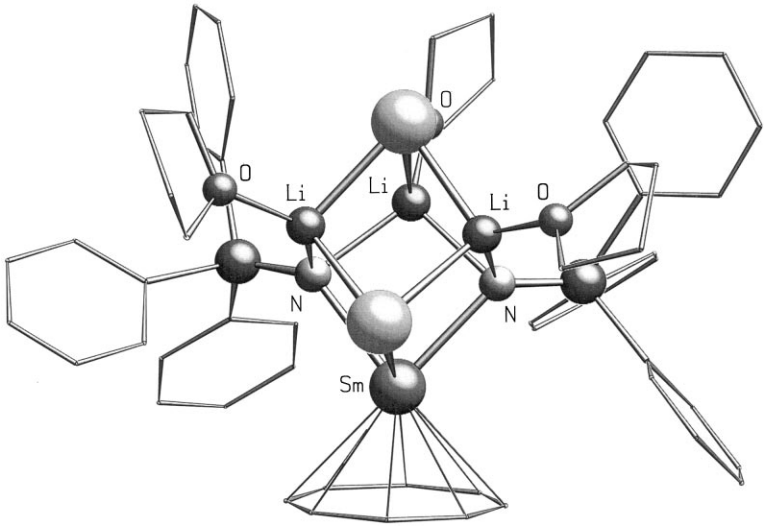

Fig. 24. View of the heterocubane structure of $[Sm(C_8H_8)Li_3Cl_2(NPPh_3)_2(THF)_3]$ [1b].

8. Oxidation state +II (Mn, Fe, Co, Ni, Cu, Zn, Cd, Mo)

Preparation, spectroscopic and structural features of phosphoraneiminato complexes of 3d elements Mn, Fe, Co, Ni, Zn as well as of mixed-valence complexes of Cu and of 4d element Cd, have been well explored in recent years. In most cases, tetrameric units with a $[M_4N_4]$ heterocubane core prevail. The nature of exocyclic ligands X in these $[MX(NPR_3)]_4$ complexes can be varied to a great extent, including halide functions, hydride ions, as well as organic substituents. On the other hand, substituents R at phosphorus are restricted to small groups such as Me or Et. No examples of derivatives with sterically demanding R groups, e.g. Ph, ^{t}Bu, cy-C_6H_{11} have been reported. Generally, heterocubane $[M_4N_4]$ cores deviate only slightly from the ideal cubic structure (Table 6). The bonding mode is of the μ_3-N-bridging type **E** with varying degrees of polarity in M–N bonds. In some cases, terminal halide functions have been replaced by carbon nucleophiles, without loss of the heterocubane structure. The preparative potential of the resulting highly reactive organometallics $[MR'(NPR_3)]_4$ for synthetic transformations in organic synthesis has so far been explored little. Equally, information is scarce as to magnetic behaviors of open-shell complexes of Mn(II), Fe(II), Co(II) and Ni(II), which all display magnetic moments lower than the corresponding spin-only values at room temperature. The colors of these heterocubanes of Mn (orange–red), Fe (brownish–black) and Co/Ni (dark green) are strikingly intense and arise from charge-transfer transitions. Molecular ions of high relative intensities can be observed in mass spectra, as well as trimeric $[MX(NPR_3)]_3^+$ and dimeric $[MX(NPR_3)]_2^+$ fragments.

First, examples of phosphoraneiminato complexes of zinc and cadmium have been observed by Schmidbaur and Jonas [70] who reacted metal dialkyls with phosphoraneimines, Eq. (17):

$$MR'_2 + HNPR_3 \rightarrow \tfrac{1}{4}[MR'(NPR_3)]_4 + R'H$$

where M = Zn, Cd; R = R′ = Me, Et (17)

Later, Klein et al. achieved the synthesis of nickel derivatives $[NiCl(NPMe_3)]_4$ and $[\{NiCl(PMe_3)\}_3(\mu_3\text{-NH})(\mu_3\text{-NPMe}_3)]$ [71] by photolysis of $[NiCl(N_3)(PMe_3)_2]$ in a toluene solution. A more rational route for the synthesis of the heterocubane has been reported by the same authors employing the azido complex $[NiCl(N_3)(PMe_3)_2]$, Eq. (18):

$$4[NiCl(N_3)(PMe_3)_2] + 4LiNPPh_3 \rightarrow [NiCl(NPMe_3)]_4 + 8PMe_3 + 4LiN_3 \quad (18)$$

A more general method for the synthesis of TM phosphoraneiminato complexes with heterocubane structure has been found in heating anhydrous metal halides with silylated phosphoraneimines Me_3SiNPR_3 at 160–220°C in the presence of a fluoride source, e.g. NaF or KF, in the melt, [72] Eq. (19):

$$MX_2 + Me_3SiNPR_3 + NaF \rightarrow \tfrac{1}{4}[MX(NPR_3)]_4 + FSiMe_3 + NaX$$

where M = Mm, Fe, Co, Ni, Zn, Cd; R = R′ = Me, Et; X = Cl, Br, I (19)

Table 6
Selected, partly average bond lengths (pm) and bond angles (°) in phosphoraneiminato complexes of Mn(II), Fe(II), Co(II), Ni(II), Cu(II), Zn(II), and Cd(II)

	M···M	M–X	M–N	P–N	M–N–M	N–M–N	Ref.
$[MnCl(NPEt_3)]_4$	297.0	230.1	213.2	158.8	88.0	92.1	[73]
$[MnBr(NPEt_3)]_4$	295.7	244.8	213.4	159.4	87.8	92.1	[74]
$[MnI(NPEt_3)]_4$	296.1	265.83	213.7	159.2	88.5	92.2	[72]
$[Mn_4Br_5\{NP(NMe_2)_3\}_3]$	292.7, 328.6	$242.6^{t\ a}$, $271.1^{br\ b}$	212.7	158.0	88.7, 99.6	92.4, 94.0	[75]
$[Mn(CH_3)(NPEt_3)]_4$	301.7	219.5	215.4	157.3	88.9	91.1	[76]
$[Mn(n\text{-}C_4H_9)(NPEt_3)]_4$	304.0	216.8	215.4	156.9	89.5	90.5	[77]
$[Mn(C\equiv C\text{–}C_6H_5)(NPEt_3)]_4$	299.3	208.0	214.5	157.9	88.5	91.5	[76]
$[Mn(C\equiv C\text{–}C_7H_7)(NPEt_3)]_4$	298.2	207.3	213.6	158.1	88.8	91.2	[76]
$[Mn(C\equiv C\text{–}SiMe_3)(NPEt_3)]_4$	298.1	207.5	214.3	157.2	88.4	91.6	[76]
$[FeCl(NPEt_3)]_4$	272.9	226.6	205.7	158.9	83.1	96.5	[74]
$[Fe_3Cl_4\{NP(NMe_2)_3\}_3]$	267.8, 295.5	224.6^{t}, 240.1^{br}	205.2^{μ_3}, 194.9^{μ_2}	158.2	86.9	94.6, 113.8	[75]
$[Fe(C\equiv C\text{–}SiMe_3)(NPEt_3)]_4$	281.4	199.2	207.7	157.0	85.5	94.4	[75]
$[CoCl(NPEt_3)]_4$	280.5	222.9	204.8	159.6	86.5	93.4	[72]
$[CoBr(NPMe_3)]_4$	280.8	236.9	203.7	158.8	87.2	92.8	[8]
$[CoBr(NPEt_3)]_4$	279.0	237.0	204.4	159.2	86.0	93.9	[8]
$[CoI(NPMe_3)]_4$	278.9	256.5	203.0	158.3	86.8	93.3	[78]
$[Co(C\equiv C\text{–}CMe_3)(NPMe_3)]_4$	284.2	197.1	204.1	157.4	88.1	91.8	[8]
$[Co(C\equiv C\text{–}SiMe_3)(NPEt_3)]_4$	281.5	195.3	204.4	159.7	87.0	92.9	[8]
$[NiCl(NPEt_3)]_4$	285.2	222.9	201.6	160.1	90.3	89.7	[73]
$[NiBr(NPMe_3)]_4$	286.9	236.3	202.1	157.9	90.5	89.5	[79]
$[NiBr(NPEt_3)]_4$	285.3	236.7	201.8	160.1	90.0	90.0	[79]
$[NiI(NPEt_3)]_4$	286.1	256.8	202.0	160.3	90.2	89.8	[79]
$[(\mu_3\text{-}NH)(\mu_3\text{-}NPMe_3)(NiClPMe_3)_3]$	263.1–265.4(1)	183.8–185.5(6) (HN-μ_3-Ni)	194.9–195.8(6)	160.9(7)	84.5–85.6(3)	–	[71]
$[Cu_4(O_2C\text{-}CH_3)_5(NPMe_3)_3]$	290–318	198.9–208.2	194.0–224.8	159.6	87.6–107.6	82.8–93.1	[80]
$[Cu_6Br_6(NPMe_3)_4]$	268.8	236.5	191.2	162.2	87.8–90.5		[81]
$[Cu_6Cl_7(NPMe_3)_4][Me_3SiNPMe_3]$	267–276	225.7^{t}, 274.4^{br}	189.3–194.8(9)	162.4	89.6		[82]
$[Cu_6Cl_6(NPMe_3)_4]^+$ $[Cu(Me_3SiNPMe_3)_2]Cl_2^-$	268–272	228.9	191.3	160.5	89.4		[82]

Table 6 (*Continued*)

	M···M	M–X	M–N	P–N	M–N–M	N–M–N	Ref.
$[ZnCl(NPMe_3)]_4$	289.2	216.5	206.3	157.3	89.0	91.0	[9]
$[ZnBr(NPMe_3)]_4$	286.1	233.7	204.7	156.8	88.7	91.4	[83]
$[ZnI(NPMe_3)]_4$	287.0	252.6	205.0	158.0	88.7	91.3	[78]
$[Zn(CH_3)(NPMe_3)]_4$	297.2	199.8	208.8	155.6	90.6	89.4	[84]
$[Zn(n\text{-}C_4H_9)(NPMe_3)]_4$	297.0	198.6	208.8	155.3	90.8	89.3	[84]
$[Zn_4(\mu_3\text{-}I)(n\text{-}C_4H_9)_4(NPMe_3)_3]$	293.3, 326.7	296.5	202.8, 212.0	158.4	107.3, 90.7	86.5, 91.2	[84]
$[Zn(C{\equiv}C\text{–}SiMe_3)(NPMe_3)]_4$	291.7	195.8	206.9	156.4	89.7	90.3	[9]
$[Zn(C{\equiv}C\text{–}C{\equiv}C\text{–}SiMe_3)(NPEt_3)]_4$	291.3	193	208.7	156.5	88.5	91.5	[9]
$[Zn(\mu_2\text{-}NPEt_3)\{N(SiMe_3)_2\}]_2$	276.5	189.1[t]	194.8[br]	156.5	90.6	89.4	[9]
$[Zn_3(\mu_2\text{-}NPMe_3)_4\{N(SiMe_3)_2\}_2]$	279.2	190.4[t]	191.7–201.8[br]	153.4, 154.5	90.4, 91.2	87.0–134.3	[9]
$[Zn_3(CH_2CN)_3(LiBr)(NPMe_3)_4]$	286.2	203	200.7, 209.7	155.8	86.7–91.0	91.6–99.6	[85]
$[CdCl(NPEt_3)]_4$	323.7	239.5	227.9	158.5	90.5	89.4	[86]
$[CdBr(NPEt_3)]_4$	321.9	249.9	225.9	159.1	90.9	89.2	[86]
$[CdI(NPEt_3)]_4$	323.8	267.7	227.0	160.0	90.7	88.8	[86]
$[Cd(C{\equiv}C\text{–}SiMe_3)(NPEt_3)]_4$	328.8	213.4	229.4	158.1	91.8	88.1	[86]
$[Cd_4I_4(NPEt_3)_3(OSiMe_3)]$	321.9, 330.2	266.9	229.4, 224.6	159.3	90.6, 94.4	88.3, 90.2	[86]

[a] t, terminal group.
[b] br, bridging group.

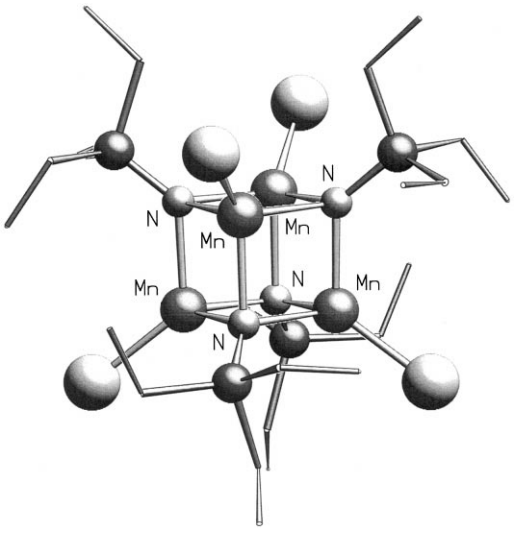

Fig. 25. Molecular structure of $[MnCl(NPEt_3)]_4$ [73].

High reaction temperatures are necessary for the metal halides and silylated phosphoraneimines form thermally stable donor–acceptor complexes of molar ratios 1:1 or 1:2 (see Section 10).

Examples of heterocubanes $[MX(NPR_3)]_4$ are illustrated in Figs. 25–30. Only in the iron compound $[FeCl(NPEt_3)]_4$ [74] a significant deviation from the ideal cubic structure has been observed, with the average Fe–N–Fe angles being 83.1°, and the

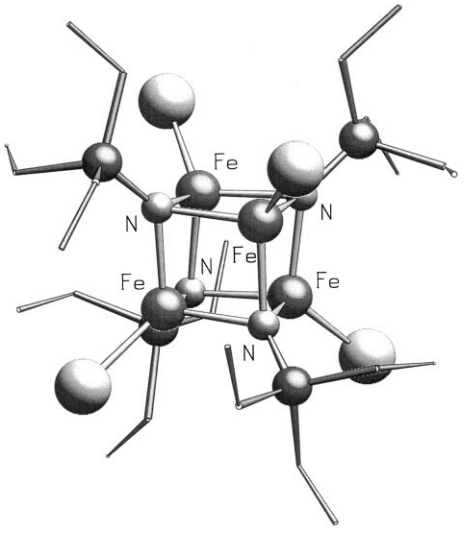

Fig. 26. Molecular structure of $[FeCl(NPEt_3)]_4$ [74].

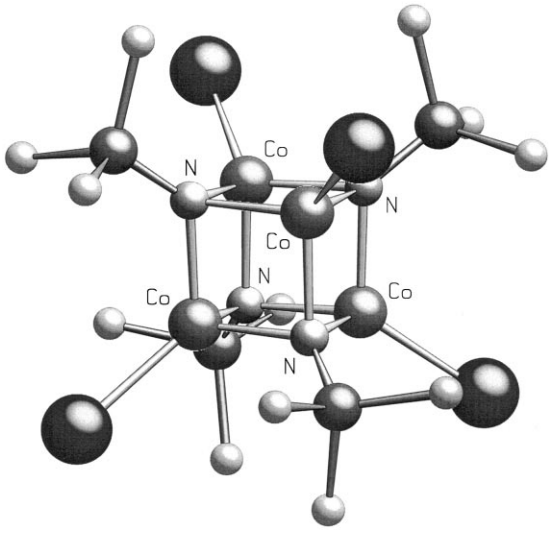

Fig. 27. Molecular structure of $[CoI(NPMe_3)_4]$ [78].

corresponding angles at nitrogen being 96.5° in average. Thus, with the Fe···Fe distances shortened (mean value 272.9 pm) bonding interactions between the metal atoms can be assumed. On the other hand, magnetic susceptibility measurements and ^{57}Fe-Mößbauer experiments do not reveal these anomalies.

In some cases, irregular heterocubanes have been isolated, in which one of the atoms of the heterocubane core $[M_4N_4]$ has been replaced by a different group. An

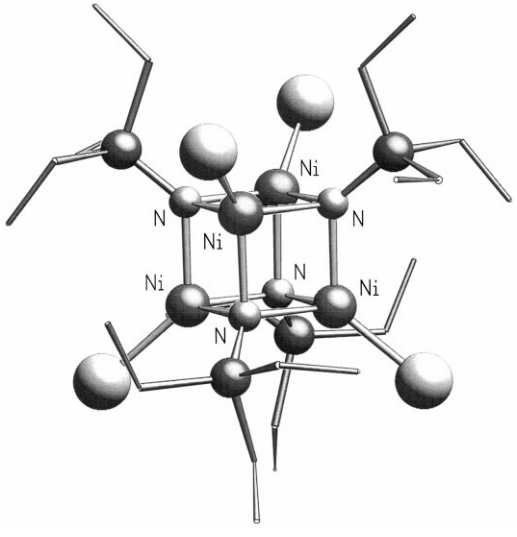

Fig. 28. Molecular structure of $[NiCl(NPEt_3)]_4$ [73].

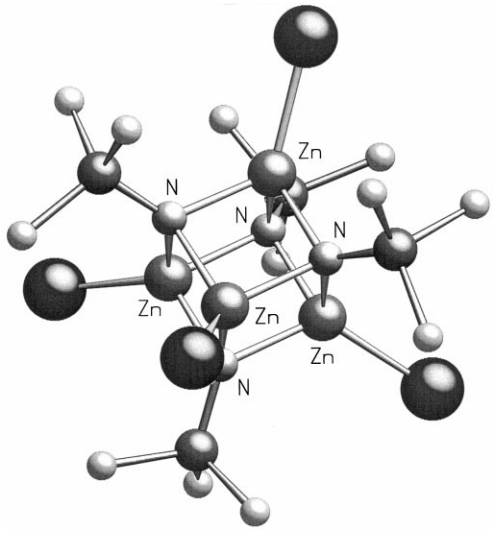

Fig. 29. Molecular structure of $[ZnI(NPMe_3)]_4$ [78].

example for replacing a μ_3-NPR_3^- function by a μ_3-halide is the bromomanganese complex $[Mn_4Br_5\{NP(NMe_2)_3\}_3]$ [75] (Fig. 31). In organozinc chemistry, both exchange of the non-metal- as well as the metal-moiety have been accomplished, examples being $[Zn_4I(^nBu)_4(NPMe_3)_3]$ [84] (Fig. 32) and the ionic complex $[Zn_3(CH_2CN)_3(BrLi)(NPMe_3)_4]$ [85], respectively. In the latter complex, one (ZnR′) vertex is replaced by a LiBr molecule, giving rise to an anionic cube (Fig. 33), the

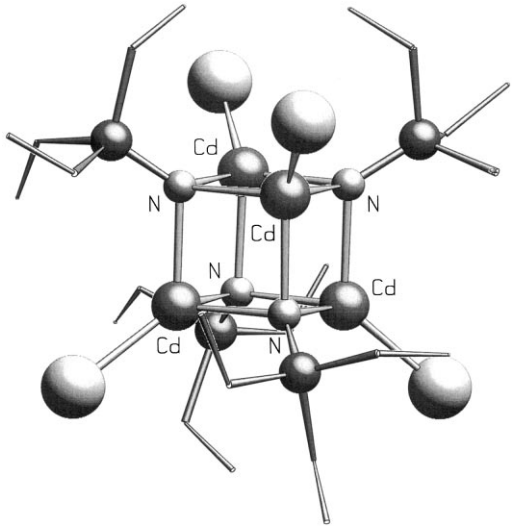

Fig. 30. Molecular structure of $[CdBr(NPEt_3)]_4$ [86].

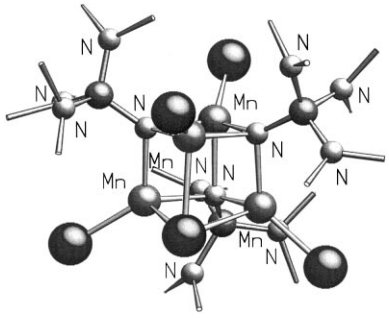

Fig. 31. View of the heterocubane-like structure of $[Mn_4Br_5\{NP(NMe_2)_3\}_3]$ [75].

charge of which is neutralized by a $[Li(THF)]^+$ cation, forming a ionic complex polymer [85]. Very recently, the crystal structure of irregular cadmium phosphoraneiminato complex $[Cd_4I_4(NPEt_3)_3(OSiMe_3)]$ has been published [86], in which one $NPEt_3^-$ ligand has been replaced by the isoelectronic silyloxy function $OSiMe_3^-$. Naturally, the exchange of one hetero-atom results in a drastic distortion of angles and bond lengths in the corresponding cube (Table 6). Employing dimethylamino groups at phosphorus, establishing a regular $[M_4N_4]$ heterocubane has not yet been achieved. On the other hand, novel preparative routes for the synthesis of very reactive, 'incomplete' cubane frameworks can be developed using the strategy of 'steric overload'. Mixed-valence $[Fe_3Cl_4\{NP(NMe_2)_3\}_3]$ [75] (Fig. 34) with three iron centres can serve as an example. According to a crystal structure determination, the site of the Fe(III) atom is not to be localized. Another example of a non-cubic three-metal centre array is derived from the regular heterocubane $[ZnBr(NPMe_3)]_4$, [83] which upon treatment with sodium bis(trimethysilyl)amide disintegrates to form $[Zn_3\{N(SiMe_3)_2\}_2(NPMe_3)_4]$ [9] (Fig. 35). In a similar reaction

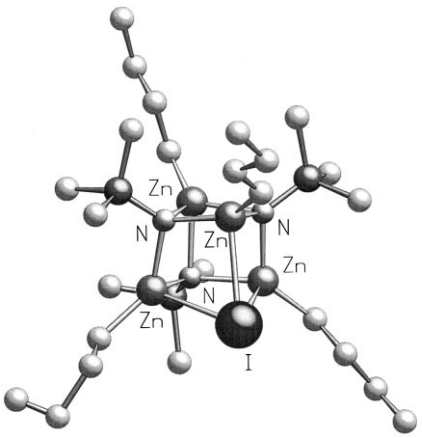

Fig. 32. View of the heterocubane-like structure of $[Zn_4I(n\text{-}Bu)_4(NPMe_3)_3]$ [84].

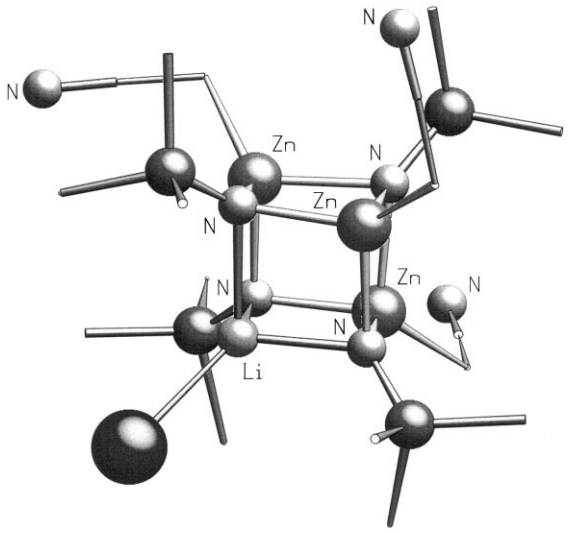

Fig. 33. View of the heterocubane-like structure of the complex anion $[Zn_3(CH_2CN)_3(LiBr)(NPMe_3)_4]^-$ [85].

employing P-ethyl bromozinc derivative $[ZnBr(NPEt_3)]_4$ steric strain leads to the formation of 'half heterocubanes' $[Zn\{N(SiMe_3)_2\}(NPMe_3)]_2$ [9]. The synthetic potential of these amidozinc phosphoraneiminato complexes has not been established yet.

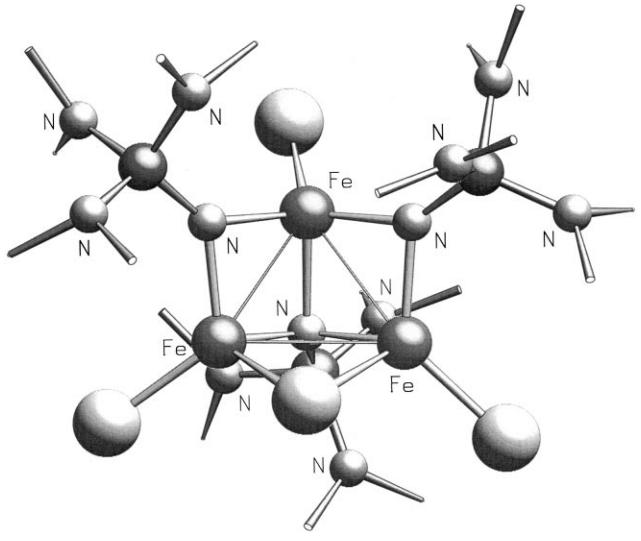

Fig. 34. Molecular structure of the mixed-valence iron complex $[Fe_3Cl_4\{NP(NMe_2)_3\}_3]$ [75].

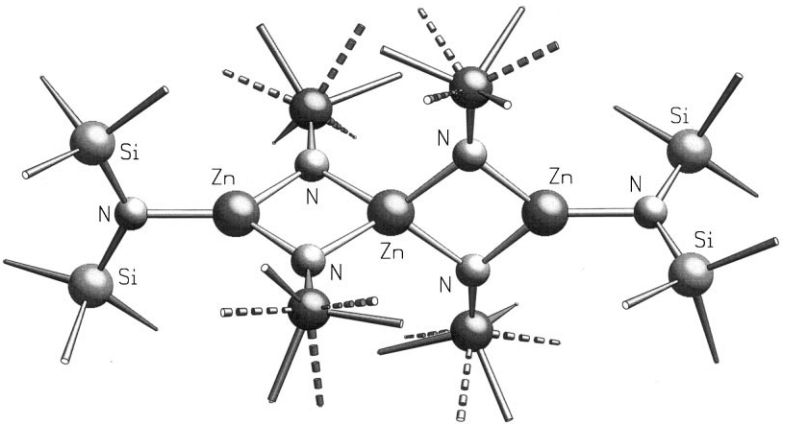

Fig. 35. Molecular structure of the amido-phosphoraneiminato complex $[Zn_3\{N(SiMe_3)_2\}_2(NPMe_3)_4]$ [9].

In the mixed-valence copper cluster $[Cu_6Br_6(NPMe_3)_4]$ [81] (containing two Cu(I) atoms, Fig. 36) delocalization of bonding electrons has also to be assumed, as is the case for the compounds $[Cu_6Cl_7(NPMe_3)_4]$ [82] (Fig. 37) and $[Cu_6Cl_6(NPMe_3)_4]^+$ [82] with one Cu(I) atom in each complex. The deep-blue clusters consist of almost regular octahedra, the μ_3-$NPMe_3^-$ ligands occupying four octahedral faces. The structure of $[Cu_6Cl_7(NPMe_3)_4]$ [82] contains an additional μ_3-bridging chloride ion.

With view of synthetic applications, it is important that halogeno-derivatives $[MX(NPR_3)]_4$ are susceptible to organometallic derivatization by reaction with

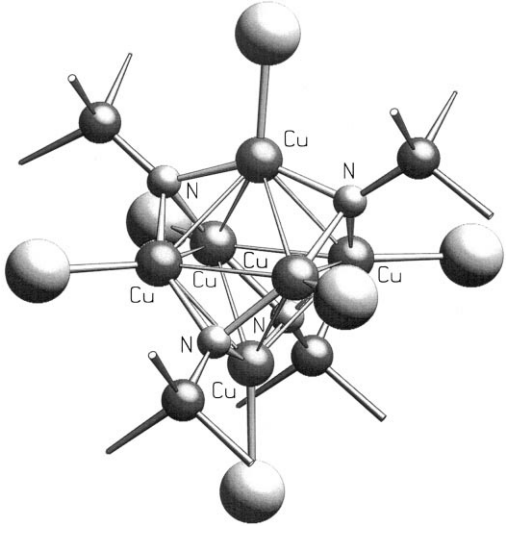

Fig. 36. Molecular structure of the mixed-valence cluster $[Cu_6Br_6(NPMe_3)_4]$ [81].

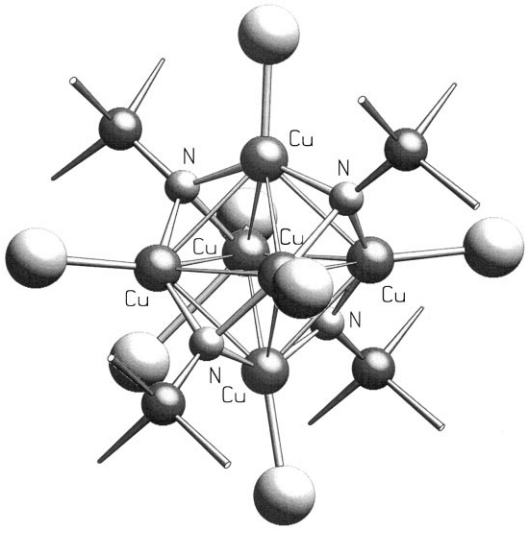

Fig. 37. Molecular structure of the mixed-valence cluster $[Cu_6Cl_7(NPMe_3)_4]$ [82].

organolithium reagents. In the case of manganese [76,77], iron [75], cobalt [8], zinc [9,84], and cadmium [86], σ-bonded organic substituents have been attached to the metal centres at the exocyclic positions, with retention of the heterocubane framework, Eq. (20):

$$[MX(NPR_3)]_4 + 4LiR' \rightarrow [MR'(NPR_3)]_4 + 4LiX \text{ where M} = \text{Mn, Fe, Co, Zn, Cd} \quad (20)$$

Interestingly, only phosphoraneiminato heterocubanes with metals of d^5-(manganese) and d^{10}-(zinc, cadmium) electron configuration are suitable for substitution with a wide range of carbon nucleophiles R′ (*n*-alkyl, alkenyl, alkynyl). It is noted that only substituents with little steric demand can be employed in these transmetallation reactions according to Eq. (20). Using Fe(II) and Co(II) complexes, substitution has only been brought about with alkynyl substituents such as $C \equiv C-R'$ ($R' = CMe_3$, $SiMe_3$). However, easy access to alkynylcobalt(II) complexes is remarkable with respect to formation of Co(II)–carbon σ-bonds. Contrary to derivatives of other metals, in electron-impact MS spectra of organocobalt species not only the molecular ions $[Co(C \equiv C-R')(NPR_3)]_4^+$ are observed in high relative intensities, but also the fragments $[Co(NPR_3)]_4^+$ and $[Co(NPR_3)]_2^+$ [8]. The required reduction of Co(II) to Co(I) is reminiscent of thermally induced homolytic cleavage of Co–C bonds in coenzyme B_{12} and methylcobalamines. Examples of structures of organometallic phosphoraneiminato heterocubanes are given in Figs. 38–42. Alternative synthetic approaches to alkynyl derivatives have been found in reacting sufficiently acidic terminal alkynes with either alkylmanganese, -zinc or -cadmium heterocubanes (Eq. (21)) or with the hydridozinc complex $[ZnH(NPMe_3)]_4$, Eq. (22) [9]:

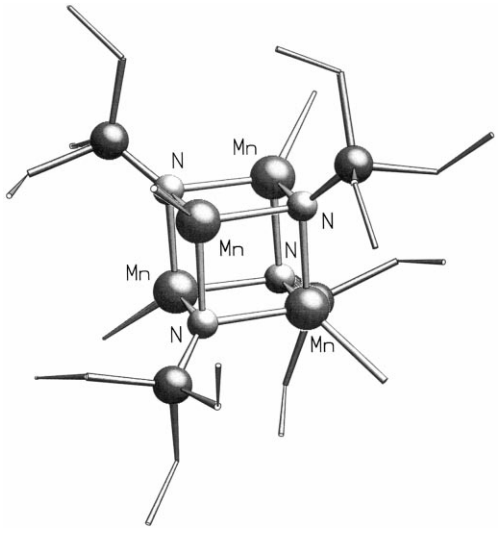

Fig. 38. Molecular structure of $[Mn(CH_3)(NPEt_3)]_4$ [76].

$$[MR'(NPR_3)]_4 + 4H{-}C \equiv C{-}R'' \rightarrow [M(C \equiv C{-}R'')(NPR_3)]_4 + 4R'H \quad (21)$$

$$[ZnH(NPMe_3)]_4 + 4H{-}C \equiv C{-}R'' \rightarrow [Zn(C \equiv C{-}R'')(NPMe_3)]_4 + 4H_2 \quad (22)$$

The follow-up chemistry of organometallic phosphoraneiminato complexes has been explored little so far, but initial experiments promise potential as mild alkylation agents. For example, treatment of P(III)-halides with organozinc com-

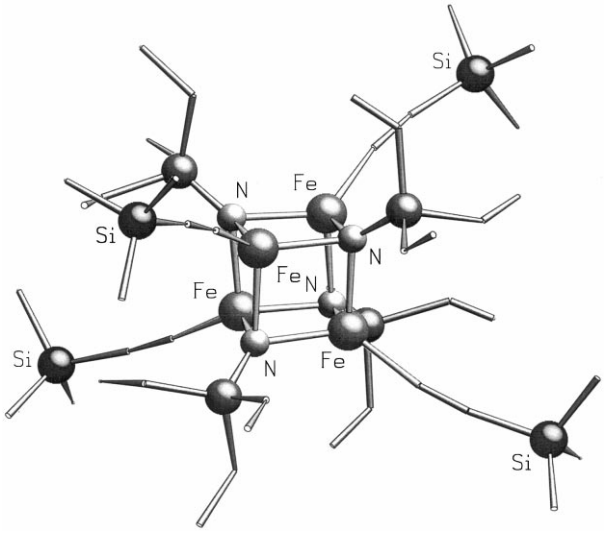

Fig. 39. Molecular structure of $[Fe(C \equiv C{-}SiMe_3)(NPEt_3)]_4$ [75].

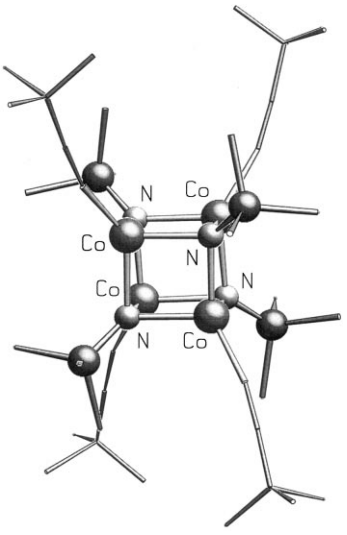

Fig. 40. Molecular structure of $[Co(C \equiv C{-}CMe_3)(NPMe_3)]_4$ [8].

plex $[ZnMe(NPMe_3)]_4$ leads to alkylation of the phosphorus component, Eq. (23) [9]:

$$[Zn(CH_3)(NPMe_3)]_4 + 4Ph_2P{-}Cl \rightarrow [ZnCl(NPMe_3)]_4 + 4Ph_2P{-}Me \quad (23)$$

C–C-bond forming reactions have also just recently been disclosed, as is illustrated with the following examples of reactions with an acrylester bromide (Eq. (24) [9]),

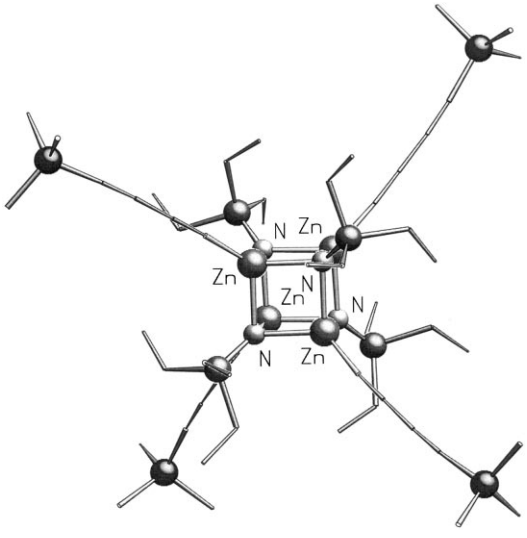

Fig. 41. Molecular structure of $[Zn(C \equiv C{-}C \equiv C{-}SiMe_3)(NPEt_3)]_4$ [9].

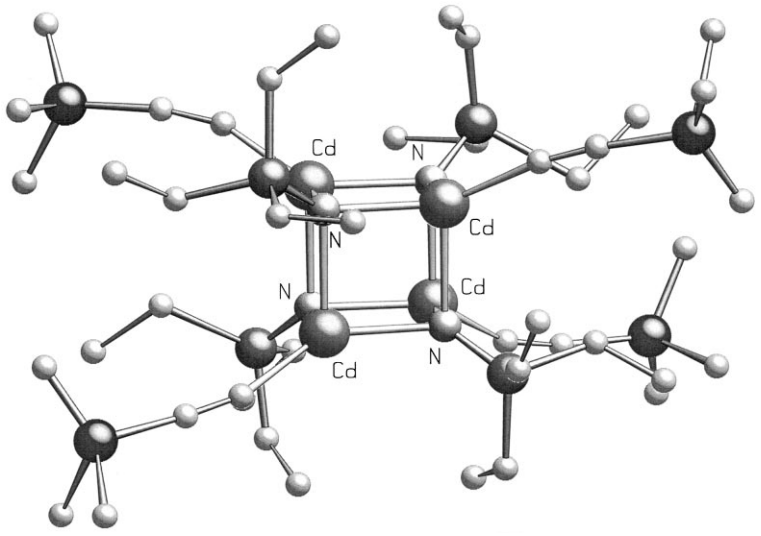

Fig. 42. Molecular structure of $[Cd(C\equiv C{-}SiMe_3)(NPEt_3)]_4$ [86].

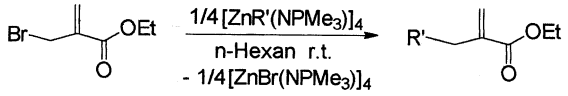

or a *Negishi*-type cross-coupling reaction which proceeds catalytically with respect to the palladium catalyst, Eq. (25) [9]:

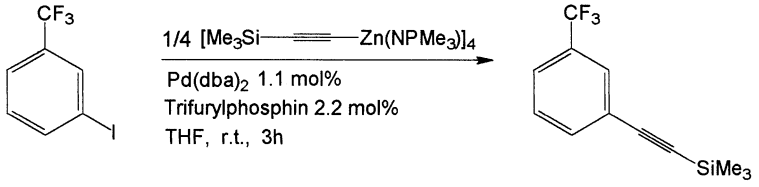

Further phosphoraneiminato derivatives of transition metals in the OS +II comprise the aforementioned hydridozinc species $[ZnH(NPMe_3)]_4$, derived from the corresponding bromozinc complex by reaction with potassium selectride, 26 [9]:

$$[ZnBr(NPMe_3)]_4 + 4KBH(^{s}Bu)_3 \rightarrow [ZnH(NPMe_3)]_4 + 4KBr \quad (26)$$

as well as amido-phosphoraneiminato complexes (see above), with the latter being further examples of lowering the symmetry by attachment of sterically demanding ligands.

Finally, it should be noted that only one example of a monomeric phosphoraneiminato complex of molybdenum in the formal OS II $[Mo(NO)(NPMePh_2)(dttd)]$ (dttd = 2,3,8,9-dibenzo-1,4,7,10-tetrathiadecane, charge $2-$) [87] has been reported. In this complex, molybdenum is shielded by the four sulfur atoms of the $dttd^{2-}$ ligand.

9. Oxidation state +I (Cu, Ag, Au)

Only few examples of phosphoraneiminato complexes of TM in the OS I have been disclosed so far. No crystal structures of Cu(I) derivatives have been described in the literature, yet during the course of examinations toward C–H activation of terminal alkynes, copper phosphoraneiminato complexes $[Cu\{NP(NMe_2)_3\}\{CuCl\}]_4$ and $[Cu\{NP(pyr)_3\}\{CuBr\}]_4$ (pyr = pyrrolidyl) have been synthesized in our group [97]. According to spectral data, and in analogy to tetrameric donor–acceptor complex $[Cu(HNPEt_3)(O_3SCF_3)]_4$, in which four Cu atoms and four μ_2-N atoms form an eight-membered ring (see Section 10), these complexes consist of Cu_4N_4 rings with a terminal (CuX) molecule bonded to the bridging N atoms.

An ionic phosphoraneiminato cluster of Ag(I) is attainable by the reaction of the heterocubane $[CoBr(NPEt_3)]_4$ with an excess of silver triflate in dichloromethane (Eq. (27)) or by heating silver triflate with silylated phosphoraneimine $Me_3SiNPEt_3$ at 140°C (Eq. (28)) [88]:

$$2[CoBr(NPEt_3)]_4 + 20Ag(O_3SCF_3) \rightarrow [Ag_{12}(NPEt_3)_8]^{4+}[OSCF_3]_4^- + 8AgBr + 8Co(O_3SCF_3)_2 \quad (27)$$

$$12Ag(O_3SCF_3) + 8Me_3SiNPEt_3 \rightarrow [Ag_{12}(NPEt_3)_8]^{4+}[O_3SCF_3]_4^- + 8Me_3SiOSO_2CF_3 \quad (28)$$

According to the structure analysis, silver atoms occupy the edges of a cube, whereas the nitrogen atoms of the $NPEt_3^-$ groups are placed at the vertices in the same way as in tetrameric heterocubane molecules, Fig. 43.

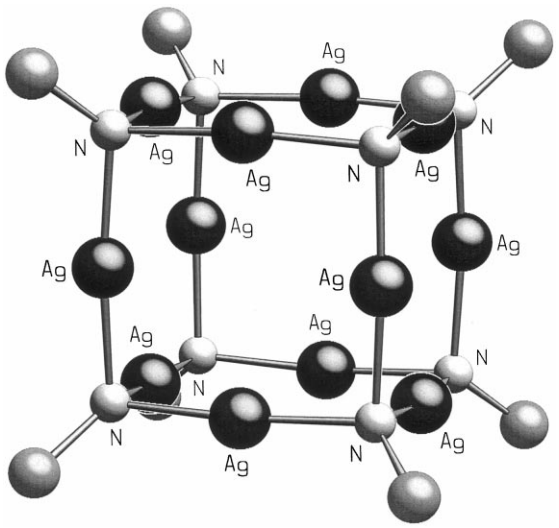

Fig. 43. View of the cation $[Ag_{12}(NPEt_3)_8]^{4+}$ in the structure of $[Ag_{12}(NPEt_3)_8]^{4+}[O_3SCF_3]_4^-$ [88]. Ethyl groups are omitted for clarity.

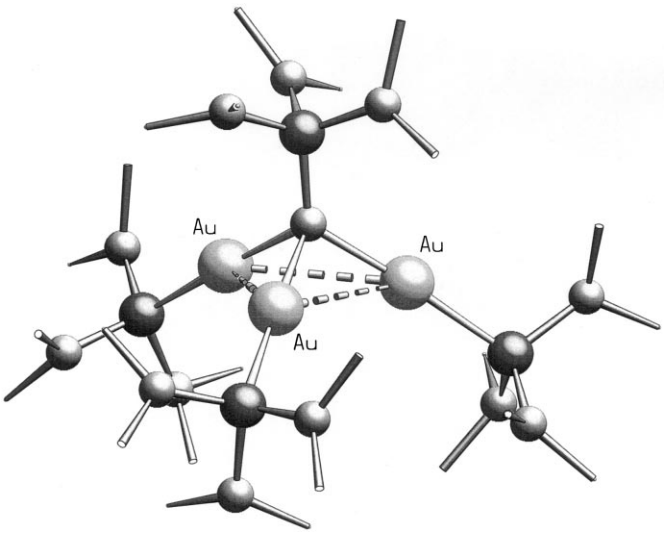

Fig. 44. Molecular structure of the complex cation $[(Me_2N)_3PN\{Au(P(NMe_2)_3)\}_3]^{2+}$ [90].

μ_3-Bridging functions of bonding mode **E** are also observed in gold(I) phosphoraneiminato complexes $[Ph_3PN\{Au(PPh_3)\}_3]^{2+}2BF_4^-$ [89] and $[(Me_2N)_3PN\{Au(P(NMe_2)_3)\}_3]^{2+}2BF_4^-$ [90] which are obtained from the corresponding oxonium compounds by adding equimolar amounts of silylated phosphoraneimines, Eq. (29):

$$[O\{Au(PR_3)\}_3]^+BF_4^- + Me_3SiNPR_3 \rightarrow [R_3PN\{Au(PR_3)\}_3]^{2+}2BF_4^- \quad (29)$$

Structures of the cations are shown in Fig. 44 using the dimethylamido derivative $[(Me_2N)_3PN\{Au(P(NMe_2)_3)\}_3]^{2+}$. Au–N distances are relatively long (209 pm in average), and the N–Au–P angles are almost linear (179.5–177.6°) [90]. Upon changing the molar ratios of the starting materials, dinuclear mono-cations can be synthesized also, Eq. (30) [89,90]:

$$2/3[O\{Au(PR_3)\}_3]^+BF_4^- + Me_3SiNPR_3 \rightarrow [R_3PN\{Au(PR_3)\}_2]^+BF_4^- \quad (30)$$

10. Donor–acceptor complexes of transition metal halides with silylated phosphaneimines

Most of the synthetic procedures for phosphoraneiminato complexes described in Sections 1–9 make use of silylated phosphoraneimines Me_3SiNPR_3 as starting materials. However, the mechanism of the reactions with TM halides and TM oxides has not yet been established. It can be assumed that the formation of donor–acceptor complexes of the type

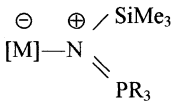

comprises the first step, followed by cleavage of trimethylsilyl halide or hexamethyldisiloxane. Indeed, stable molecular complexes of some metal halides can be isolated, which upon thermolysis, and eventually, presence of alkaline fluorides, are transformed into phosphoraneiminato complexes. Most numerous complexes of the donor–acceptor type have been described of metal(II) halides, and Fe(III) and Zr(IV) both contribute one example (see Table 7). Complexes of particularly strong Lewis-acids, amongst others $TiCl_4$, $NbCl_5$, $TaCl_5$ and $MoCl_5$, as well as WF_6 and WCl_6, are unknown to date. Elongation of the Si–N bond of the coordinating phosphoraneimine molecule should be favourable for the cleavage of the trimethylsilyl halide from the donor–acceptor complexes. However, crystal structure analyses generally reveal only an insignificant change in Si–N bond distances, compared with those in uncoordinated phosphoraneimines [4]. Exceptions from this are the complexes $[FeCl_3(Me_3SiNPEt_3)]$ [63] and $[ZrCl_4(Me_3SiNPPh_3)]$ [56], with Si–N bonds as long as 177.9 and 179.4 pm, respectively. Still, even at temperatures above 200°C, zirconium complex $[ZrCl_4(Me_3SiNPPh_3)]$ is not viable to decomposition, whereas from iron derivative $[FeCl_3(Me_3SiNPEt_3)]$ trimethylsilylchloride is dissociated in boiling dichloromethane already. These results show that no uniform mechanism can be proposed at present.

Characteristic structure examples of phosphoraneimine donor–acceptor complexes can be seen in Figs. 45–48. From these, it is obvious that the silylated phosphoraneimine molecules bind in a terminal fashion without exception. In complexes of Cr(II) and Pd(II) with planar coordination around the metal centres (1:2 stoichiometry), phosphoraneimine molecules are located in *trans* positions. In complexes with tetrahedral environment at the metal centres (Co(II), Mn(II)) N–M–N bond angles have been found to be very large (Table 7) due to steric

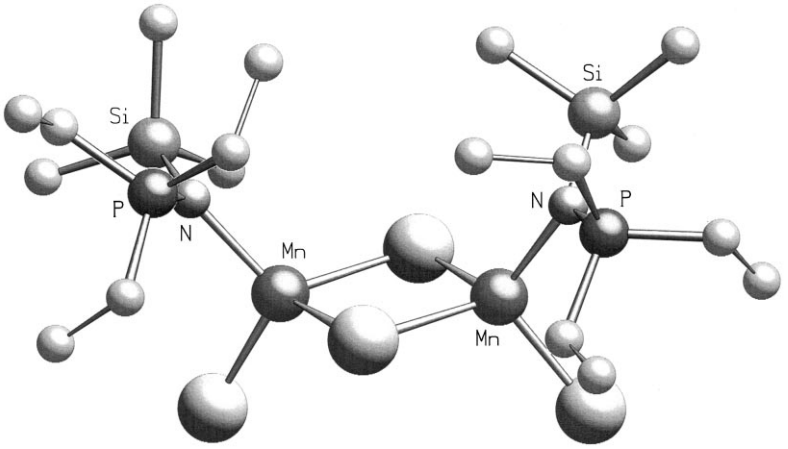

Fig. 45. Molecular structure of $[MnCl_2(Me_3SiNPEt_3)]_2$ [94].

Table 7
Selected, partly averaged bond lengths (pm) and bond angles (°) in phosphoraneimine complexes of transition-metal halides

	M–N	M–X	Si–N	P–N	N–M–N	Si–N–P	Ref.
$[ZrCl_4(Me_3SiNPPh_3)]$	216.8(2)	228.23-243.17(8)	179.4(2)	161.5(2)	–	122.4(1)	[56]
$[Zr_2OCl_6(Me_3SiNPMe_3)_2]$	217.4	244.2					[91]
$[CrCl_2(Me_3SiNPMe_3)_2]$	211.7(2)	235.94(9)	171.6(3)	158.6(3)	180	127.4(2)	[92]
$[MnCl_2(Me_3SiNPEt_3)]_2$	209.3	231.1(2)^{t} [a], 244.2^{br} [b]	173.3	160.2	–	126.9	[94]
$[MnI_2(Me_3SiNPEt_3)_2]$	220.7(13)	276.8(2)	172.1	160.7	123.1(7)	126.7	[94]
$[ReO(OSiMe_3)_3(Me_3SiNPEt_3)]$	214.0(8)	165.6(9), 194.0(8)	175.5(9)	161.2(8)	–	129.1(5)	[12]
$[FeCl_3(Me_3SiNPEt_3)]$	197.4	219.9	177.9	163.2	–	125.7	[63]
$[FeCl_2(Me_3SiNPEt_3)]_2$	202.2	224.7^{t}, 240.9^{br}	174.1	161.2	–	128.8	[63]
$[CoCl_2(Me_3SiNPMe_3)_2]$	205.5	228.8	173.5	160.5	121.4(2)	124.7	[95]
$[CoCl_2(HNPMe_3)_2]$	199.4	231.1	–	160.0	111.8(3)	–	[95]
$[Me_3SiN(H)PMe_3]^{+}[NiBr_3(Me_3SiNPMe_3)]^{-}$	202.0(3)	241.6	173.1(3)	159.3(3)	–	127.8(2)	[96]
$[NiBr_2\{HNP(NMe_2)_3\}_2]$	195.0(3)	244.16(5)	–	159.1(3)		–	[97]
$[PdCl_2(Me_3SiNPEt_3)_2]$	209.5(2)	229.9(1)	173.5(3)	159.8(3)	180	126.3(1)	[92]
$[CuCl(Me_3SiNPPh_3)]$							
$[CuCl_2(Me_3SiNPPh_3)]_2$	198.5(2)	221.4(1)^{t}, 230^{br}	175.1(3)	159.8(3)	–	127.0(2)	[93]
$[CuCl_2(Me_3SiNPMe_3)]_2$	196.7(3)	219.9(1)^{t}, 231.4^{br}	173.6(3)	159.7(3)	–	128.5(2)	[92]
$[Cu(HNPEt_3)]_4^{4+}(O_3SCF_3^{-})_4$	191.6(4), 192.1(4)	–	–	165.4(4)	167.98(9)	–	[97]
$[ZnCl_2(Me_3SiNPMe_3)_2]$	205.5	230.4	173.5	160.5	120.6(1)	124.7	[95]
$[ZnCl_2(Me_3SiNP(CH_2)_4CMe_3)]_2$	198.7(2)	220.9(1)^{t}, 236.8^{br}	174.8(2)	160.8(2)	–	126.2(1)	[83]
$[ZnI_2(Me_3SiNPEt_3)]_2$	199.0(6)	255.96(9)^{t}, 269.7^{br}	176.2(6)	160.7(5)	–	127.9(4)	[83]

[a] t, terminal group.
[b] br, bridging group.

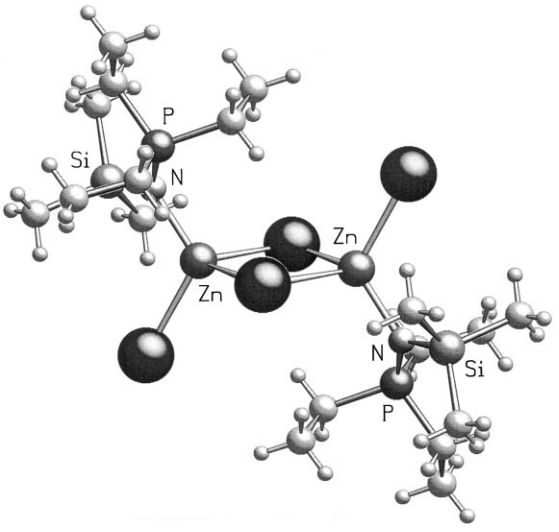

Fig. 46. Molecular structure of $[ZnI_2(Me_3SiNPEt_3)]_2$ [83].

repulsion of the phosphoraneimine ligands. In contrast to this, 1:1 complexes realise dimeric units which are associated via μ_2-halide bridges. Phosphoraneimine ligands assume *cisoid* positions in manganese compound $[MnCl_2(Me_3SiNPEt_3)]_2$ (Fig. 45 [94]), whereas the corresponding iron and zinc dimers, e.g. $[ZnI_2(Me_3SiNPEt_3)]_2$ (Fig. 46 [83]) are *transoid* with respect to the coordinated silylated phosphoraneimine molecules.

Different structural motifs are realized in complexes of $HNPR_3$ molecules

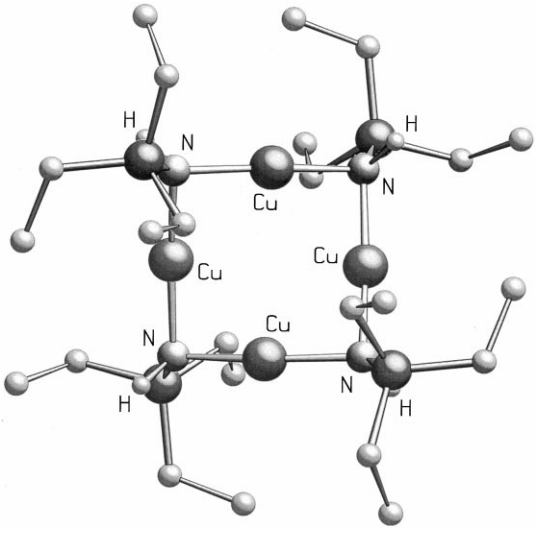

Fig. 47. View of the cation $[Cu(HNPEt_3)]_4^{4+}$ in the structure of $[Cu(HNPEt_3)(O_3SCF_3)]_4$ [97].

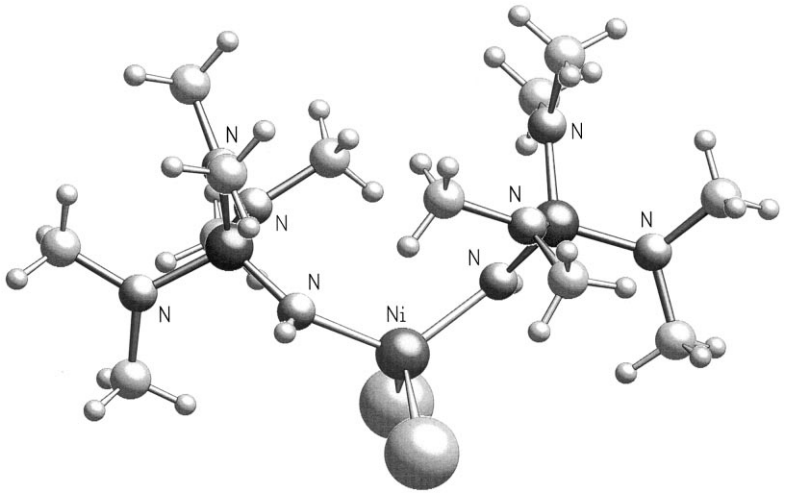

Fig. 48. Molecular structure of $[NiBr_2\{HNP(NMe_2)_3\}_2]$ [97].

coordinated at TM centres. For instance, in the aforementioned complexes $[Zr_2Cl_4(NPMe_3)_4(HNPMe_3)]$ [55] and $[Cu(HNPEt_3)(O_3SCF_3)]_4$ [97] $HNPR_3$ moieties assume μ_2-bridging positions. As described above, the four μ_2-N atoms and the four Cu(I) centres form an eight-membered Cu_4N_4 ring (Fig. 47). In contrast, two $HNP(NMe_2)_3$ molecules are coordinated terminally in monomeric C_2–symmetric nickel complex $[NiBr_2\{HNP(NMe_2)_3\}_2]$ (Fig. 48 [97]).

Acknowledgements

K.D. thanks the co-workers who contributed to the quoted publications for their commitment and efforts in the laboratories. M.K. thanks the Stiftung Stipendienfonds of the Verband der Chemischen Industrie for a doctoral fellowship. We thank Mrs U. Siepe for the careful arrangement of the manuscript. Finally, we are indebted to the Deutsche Forschungsgemeinschaft (DFG) and to the Fonds der Chemischen Industrie for their generous financial support.

References

[1] (a) A.S. Batsanov, M.G. Davidson, J.A.K. Howard, S. Lamb, C. Lustig, R.D. Price, J. Chem. Soc. Chem. Commun. (1997) 1211. (b) S. Anfang, G. Seybert, K. Harms, G. Geiseler, W. Massa, K. Dehnicke, Z. Anorg. Allg. Chem. 624 (1998) 1187.
[2] T. Miekisch, Dissertation, Universität Marburg, 1997.
[3] S. Chitsaz, B. Neumüller, K. Dehnicke, Z. Anorg. Allg. Chem. 624 (1998) in press.
[4] K. Dehnicke, F. Weller, Coord. Chem. Rev. 158 (1997) 103.
[5] K. Dehnicke, J. Strähle, Polyhedron 8 (1989) 707.
[6] D. Nusshär, F. Weller, A. Neuhaus, G. Frenking, K. Dehnicke, Z. Anorg. Allg. Chem. 615 (1992) 86.

[7] C. Mast, S. Anfang, K. Dehnicke, A. Greiner, unpublished results (1997).
[8] U. Riese, K. Harms, B. Neumüller, K. Dehnicke, Z. Anorg. Allg. Chem. 624 (1998) 1279.
[9] M. Krieger, R.O. Gould, B. Neumüller, K. Harms, K. Dehnicke, Z. Anorg. Allg. Chem. 624 (1998) 1434.
[10] K.V. Katti, H.W. Roesky, M. Rietzel, Z. Anorg. Allg. Chem. 553 (1987) 123.
[11] H.W. Roesky, D. Hesse, M. Rietzel, M. Noltemeyer, Z. Naturforsch. 45b (1990) 72.
[12] S. Schlecht, G. Geiseler, K. Harms, M. Bickelhaupt, M. Diedenhofen, K. Dehnicke, Z. Anorg. Allg. Chem. 624 (1998) in press.
[13] F. Weller, H.-C. Kang, W. Massa, T. Rübenstahl, F. Kunkel, K. Dehnicke, Z. Naturforsch. 50b (1995) 1050.
[14] M. Möhlen, N. Faza, W. Massa, K. Dehnicke, unpublished results (1997).
[15] I. Leichtweis, R. Hasselbring, H.W. Roesky, M. Noltemeyer, A. Herzog, Z. Naturforsch. 48b (1993) 1234.
[16] H.W. Roesky, K.V. Katti, U. Seseke, U. Scholz, R. Herbst, E. Egert, et al., Z. Naturforsch. 41b (1986) 1509.
[17] H.W. Roesky, U. Seseke, M. Noltemeyer, P.G. Jones, G.M. Sheldrick, J. Chem. Soc. Dalton Trans. (1986) 1309.
[18] C.H. Honeyman, A.J. Lough, I. Manners, Inorg. Chem. 33 (1994) 2988.
[19] E. Rentschler, D. Nusshär, F. Weller, K. Dehnicke, Z. Anorg. Allg. Chem. 619 (1993) 999.
[20] D. Nusshär, F. Weller, K. Dehnicke, Z. Anorg. Allg. Chem. 619 (1993) 507.
[21] M. Rhiel, S. Wocadlo, W. Massa, K. Dehnicke, Z. Naturforsch. 51b (1996) 1419.
[22] D. Nusshär, F. Weller, K. Dehnicke, Z. Anorg. Allg. Chem. 619 (1993) 1121.
[23] W.A. Nugent, J.M. Mayer, Metal–Ligand Multiple Bonds, Wiley, New York, 1988.
[24] K. Dehnicke, J. Strähle, Angew. Chem. Int. Ed. Engl. 31 (1992) 955.
[25] H.W. Roesky, I. Leichtweis, M. Noltemeyer, Inorg. Chem. 32 (1993) 5102.
[26] H.W. Roesky, F. Schrumpf, M. Noltemeyer, Z. Naturforsch. 44b (1989) 35.
[27] E. Schweda, K.D. Scherfise, K. Dehnicke, Z. Anorg. Allg. Chem. 528 (1985) 117.
[28] A. Aistars, R.J. Doedens, N.M. Doherty, Inorg. Chem. 33 (1994) 4360.
[29] H. Bezler, J. Strähle, Z. Naturforsch. 34b (1979) 1199.
[30] I. Leichtweis, H.W. Roesky, M. Noltemeyer, H.-G. Schmidt, Z. Naturforsch. 46b (1991) 425.
[31] H.W. Roesky, J. Liebermann, M. Noltemeyer, H.-G. Schmidt, Chem. Ber. 122 (1989) 1641.
[32] G. Philipp, K. Harms, K. Dehnicke, C. Maichle-Mössmer, U. Abram, Z. Anorg. Allg. Chem. 622 (1996) 1927.
[33] D. Nusshär, F. Weller, K. Dehnicke, W. Hiller, J. Alloys Compd. 183 (1992) 30.
[34] F. Weller, D. Nusshär, K. Dehnicke, Z. Anorg. Allg. Chem. 615 (1992) 7.
[35] H. Bezler, J. Strähle, Z. Naturforsch. 38b (1983) 317.
[36] K. Hösler, F. Weller, K. Dehnicke, Z. Naturforsch. 42b (1987) 1563.
[37] K. Völp, F. Weller, K. Dehnicke, Z. Naturforsch. 42b (1987) 947.
[38] G. Philipp, S. Wocadlo, W. Massa, K. Dehnicke, D. Fenske, C. Maichle-Mössmer, et al., Z. Naturforsch. 50b (1995) 1.
[39] J.R. Dilworth, B.D. Neaves, J.P. Hutchinson, J.A. Zubieta, Inorg. Chim. Acta 65 (1982) 223.
[40] H.W. Roesky, in: H.W. Roesky (Ed.), Rings, Clusters and Polymers of Main Group and Transition Elements, Elsevier, Amsterdam, 1989, p. 369.
[41] F. Weller, D. Nusshär, K. Dehnicke, F. Gingl, J. Strähle, Z. Anorg. Allg. Chem. 602 (1991) 7.
[42] J.-S. Li, M. Stahl, N. Faza, W. Massa, K. Dehnicke, Z. Anorg. Allg. Chem. 623 (1997) 1035.
[43] T. Rübenstahl, D. Wolff von Gudenberg, F. Weller, K. Dehnicke, H. Goesmann, Z. Naturforsch. 49b (1994) 15.
[44] F. Weller, F. Schmock, K. Dehnicke, Z. Naturforsch. 51b (1996) 1359.
[45] T. Rübenstahl, F. Weller, K. Harms, K. Dehnicke, D. Fenske, G. Baum, Z. Anorg. Allg. Chem. 620 (1994) 1741.
[46] M.M. Stahl, N. Faza, W. Massa, K. Dehnicke, Z. Anorg. Allg. Chem. 624 (1998) 209.
[47] R. Hasselbring, I. Leichtweis, M. Noltemeyer, H.W. Roesky, H.-G. Schmidt, A. Herzog, Z. Anorg. Allg. Chem. 619 (1993) 1543.
[48] T. Rübenstahl, F. Weller, S. Wocadlo, W. Massa, K. Dehnicke, Z. Anorg. Allg. Chem. 621 (1995) 953.

[49] T. Miekisch, K. Harms, S. Wocadlo, W. Massa, B. Neumüller, C. Frommen, K. Dehnicke, Z. Naturforsch. 52b (1997) 1484.
[50] M. Grün, K. Harms, R. Meyer zu Köcker, K. Dehnicke, H. Goesmann, Z. Anorg. Allg. Chem. 622 (1996) 1091.
[51] I.A. Latham, G.J. Leigh, G. Huttner, I. Jibril, J. Chem. Soc. Dalton Trans. (1986) 377.
[52] J.-S. Li, F. Weller, F. Schmock, K. Dehnicke, Z. Anorg. Allg. Chem. 621 (1995) 2097.
[53] R. Wollert, S. Wocadlo, K. Dehnicke, H. Goesmann, D. Fenske, Z. Naturforsch. 47b (1992) 1386.
[54] N. Kuhn, R. Fawzi, M. Steimann, J. Wiethoff, Z. Anorg. Allg. Chem. 623 (1997) 769.
[55] M.M. Stahl, N. Faza, W. Massa, K. Dehnicke, Z. Anorg. Allg. Chem. 623 (1997) 1855.
[56] M. Grün, F. Weller, K. Dehnicke, Z. Anorg. Allg. Chem. 623 (1997) 224.
[57] A. Hills, D.L. Hughes, G.J. Leigh, R. Prieto-Alcón, J. Chem. Soc. Dalton Trans. (1993) 3609.
[58] T. Rübenstahl, K. Dehnicke, H. Krautscheid, Z. Anorg. Allg. Chem. 619 (1993) 1023.
[59] T. Rübenstahl, K. Dehnicke, J. Magull, Z. Anorg. Allg. Chem. 621 (1995) 1218.
[60] F.L. Phillips, A.C. Skapski, J. Chem. Soc. Dalton Trans. (1976) 1448.
[61] R.E. Cramer, F. Edelmann, A.L. Mori, S. Roth, J.W. Gilje, K. Tatsumi, et al., Organometallics 7 (1988) 841.
[62] H.W. Roesky, U. Seseke, M. Noltemeyer, G.M. Sheldrick, Z. Naturforsch. 43b (1988) 1130.
[63] H.-J. Mai, S. Wocadlo, H.-C. Kang, W. Massa, K. Dehnicke, C. Maichle-Mössmer, et al., Z. Anorg. Allg. Chem. 621 (1995) 705.
[64] N. Mronga, F. Weller, K. Dehnicke, Z. Anorg. Allg. Chem. 502 (1983) 35.
[65] S. Anfang, K. Harms, F. Weller, O. Borgmeier, H. Lueken, H. Schilder, et al., Z. Anorg. Allg. Chem. 624 (1998) 150.
[66] S. Anfang, K. Harms and K. Dehnicke, unpublished results (1998).
[67] N.J. Long, Metallocenes, Blackwell, Oxford, 1998.
[68] K.O. Hodgson, K.N. Raymond, Inorg. Chem. 11 (1972) 171.
[69] K.O. Hodgson, F. Mares, D.F. Starks, K.N. Raymond, A. Streitwieser, Jr., G.Z. Qi, et al., in: W.A. Herrmann (Ed.), F.T. Edelmann (Vol.-Ed.), Herrmann/Brauer, Synthetic Methods of Organometallic and Inorganic Chemistry, Vol. 6, Thieme-Verlag, Stuttgart, 1997, p. 118–120.
[70] H. Schmidbaur, G. Jonas, Chem. Ber. 101 (1968) 1271.
[71] H.-F. Klein, S. Haller, H. König, M. Dartiguenave, Y. Dartiguenave, M.J. Menu, J. Am. Chem. Soc. 113 (1991) 4673.
[72] H.-J. Mai, R. Meyer zu Köcker, S. Wocadlo, W. Massa, K. Dehnicke, Angew. Chem. Int. Ed. Engl. 34 (1995) 1235.
[73] H.-J. Mai, H.-C. Kang, S. Wocadlo, W. Massa, K. Dehnicke, Z. Anorg. Allg. Chem. 621 (1995) 1963.
[74] U. Riese, N. Faza, K. Harms, W. Massa, B. Neumüller, K. Dehnicke, Phosphorus Sulfur Silicon 124 (1997) 315.
[75] U. Riese, Dissertation, Universität Marburg, 1998.
[76] U. Riese, B. Neumüller, N. Faza, W. Massa, K. Dehnicke, Z. Anorg. Allg. Chem. 623 (1997) 351.
[77] H.-J. Mai, B. Neumüller, K. Dehnicke, Z. Naturforsch. 51b (1996) 433.
[78] S. Abram, U. Abram, R. Meyer zu Köcker, K. Dehnicke, Z. Anorg. Allg. Chem. 622 (1996) 867.
[79] M. Krieger, R.O. Gould, J. Pebler, K. Dehnicke, Z. Anorg. Allg. Chem. 624 (1998) 781.
[80] R. Meyer zu Köcker, J. Pebler, C. Friebel, K. Dehnicke, D. Fenske, Z. Anorg. Allg. Chem. 621 (1995) 1311.
[81] R. Meyer zu Köcker, K. Dehnicke, D. Fenske, Z. Naturforsch. 49b (1994) 987.
[82] R. Meyer zu Köcker, A. Behrendt, K. Dehnicke, D. Fenske, Z. Naturforsch. 49b (1994) 301.
[83] M. Krieger, K. Harms, J. Magull, K. Dehnicke, Z. Naturforsch. 52b (1997) 243.
[84] M. Krieger, R.O. Gould, K. Harms, S. Parsons, K. Dehnicke, Chem. Ber. 129 (1996) 1621.
[85] M. Krieger, R.O. Gould, K. Dehnicke, unpublished results (1997).
[86] K. Harms, J. Merle, C. Maichle-Mössmer, W. Massa, M. Krieger, Inorg. Chem. 37 (1998) 1099.
[87] D. Sellmann, J. Keller, M. Moll, C.F. Campana, M. Haase, Inorg. Chim. Acta 141 (1988) 243.
[88] U. Riese, N. Faza, W. Massa, K. Dehnicke, unpublished results (1998).
[89] A. Bauer, F.P. Gabbaï, A. Schier, H. Schmidbaur, Philos. Trans. R. Soc. Lond. A354 (1996) 381.

[90] A. Bauer, N.W. Mitzel, A. Schier, D.W.H. Rankin, H. Schmidbaur, Chem. Ber./Recueil 130 (1997) 323.
[91] T. Rübenstahl, F. Weller, K. Dehnicke, Z. Kristallogr. 210 (1995) 385.
[92] T. Miekisch, H.-J. Mai, R. Meyer zu Köcker, K. Dehnicke, J. Magull, H. Goesmann, Z. Anorg. Allg. Chem. 622 (1996) 583.
[93] D. Fenske, E. Böhm, K. Dehnicke, J. Strähle, Z. Naturforsch. 43b (1988) 1.
[94] H.-J. Mai, S. Wocadlo, W. Massa, F. Weller, K. Dehnicke, C. Maichle-Mössmer, et al., Z. Naturforsch. 50b (1995) 1215.
[95] R. Meyer zu Köcker, G. Frenzen, B. Neumüller, K. Dehnicke, J. Magull, Z. Anorg. Allg. Chem. 620 (1994) 431.
[96] M. Krieger, F. Weller, K. Dehnicke, Z. Kristallogr. NCS 213 (1998) 511.
[97] M. Krieger, Dissertation, Universität Marburg, 1997.
[98] A. Dietrich, B. Neumüller, K. Dehnicke, unpublished results (1998).